

# PRV

PATENT- OCH REGISTRERINGSVERKET  
Patentavdelningen

REC'D 16 FEB 2005

WIPO

PCT

PCT / SE 2005 / 0 0 0 98

## Intyg Certificate

Härmed intygas att bifogade kopior överensstämmer med de handlingar som ursprungligen ingivits till Patent- och registreringsverket i nedannämnda ansökan.

This is to certify that the annexed is a true copy of the documents as originally filed with the Patent- and Registration Office in connection with the following patent application.



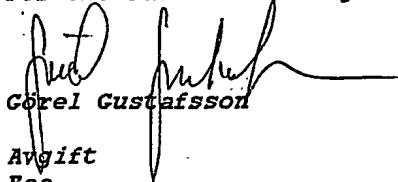
(71) Sökande                      Nanofactory Instruments AB, Göteborg SE  
Applicant (s)

(21) Patentansökningsnummer    0400177-2  
Patent application number

(86) Ingivningsdatum              2004-01-26  
Date of filing

Stockholm, 2005-02-01

För Patent- och registreringsverket  
For the Patent- and Registration Office

  
Görel Gustafsson  
Avgift  
Fee

**PRIORITY DOCUMENT**  
SUBMITTED OR TRANSMITTED IN  
COMPLIANCE WITH  
RULE 17.1(a) OR (b)

**PATENT- OCH  
REGISTRERINGSVERKET  
SWEDEN**

Postadress/Adress  
Box 5055  
S-102 42 STOCKHOLM

Telefon/Phone  
+46 8 782 25 00  
Vx 08-782 25 00

Telex  
17978  
PATOREG S

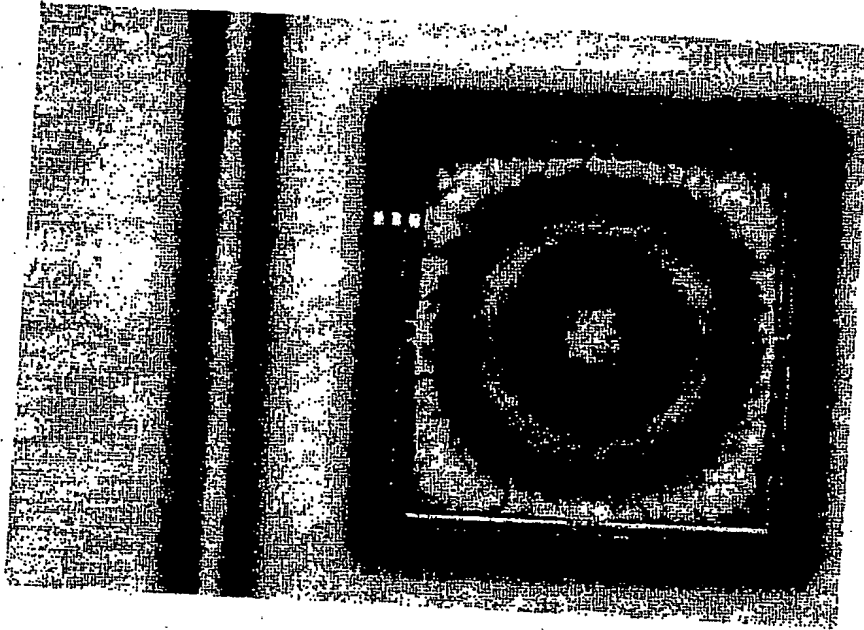
Telefax  
+46 8 666 02 86  
08-666 02 86

Ink. t. Patent- och reg.ve

2004 -01- 2 6

Huvudfaxen Kassar.

## Preliminary Report



## A Micromachined Nanoindenter Force Sensor

**Alexandra Nafari**

Department of Microelectronics  
Solid State Electronics Laboratory  
CHALMERS UNIVERSITY OF TECHNOLOGY  
Göteborg, Sweden 2004

**CONTENTS**

<b>Abstract.....</b>	<b>2</b>
<b>1 Introduction .....</b>	<b>5</b>
1.1 Background.....	5
1.2 Methodology.....	5
1.3 Sensor Specification and Requirements.....	6
<b>2 Overview of Techniques Used in Combination with the Sensor ..</b>	<b>7</b>
2.1 Transmission Electron Microscope.....	7
2.2 Nanoindentation experiments.....	8
2.3 Atomic Force Microscopy.....	9
<b>3 Force Measurements .....</b>	<b>10</b>
3.1 Capacitive Sensing .....	11
3.2 Piezoresistiv Sensing.....	11
<b>4 Design and Calculation.....</b>	<b>12</b>
4.1 Initial Nanoindenter Sensor Simulation .....	12
4.1.1 Capacitive Model Simulation.....	12
4.1.2 Piezoresistive Model Simulation.....	13
4.1.3 Final Nanoindenter Sensor Design.....	14
4.2 AFM Simulations .....	17
4.3 Motivation of Chosen Design.....	18
<b>5 Manufacturing .....</b>	<b>18</b>
5.1 Device structure.....	19
5.2 Mask design.....	19
5.2.1 Alignment marks .....	20
5.3 Performed process steps .....	20
5.3.1 Oxidation .....	21
5.3.2 Boron Doping .....	21
5.3.3 Lithography.....	21
5.3.4 Dry etching .....	22
5.3.5 Glass etch.....	23
5.3.6 Metal deposition .....	23
5.3.7 Anodic bonding .....	23
5.4 Process Comments.....	25
5.4.1 Oxide mask enhancement.....	25

5.4.2	Dry etch problems.....	25
5.4.3	Glass processing .....	26
<b>6</b>	<b>Evaluation .....</b>	<b>26</b>
6.1	CV-measurements .....	27
<b>7</b>	<b>Conclusions.....</b>	<b>29</b>
<b>8</b>	<b>Recommendation for Further work .....</b>	<b>29</b>
<b>9</b>	<b>Acknowledgements .....</b>	<b>30</b>
<b>10</b>	<b>References.....</b>	<b>31</b>
Appendix 1	CAD-drawings of the holder.....	
Appendix 2	Design layout.....	
Appendix 3	Anodic bonding.....	
Appendix 4	AFM and nanoindenter sensor calculation programs.. .....	
Appendix 5	Process Plan for a Nanoindenter Force Sensor.....	

## 1 Introduction

MEMS stands for Microelectromechanical Systems, a manufacturing technology used to produce electromechanical systems using batch fabrication techniques similar to those in IC manufacturing. MEMS integrates mechanical structures, such as sensors and actuators, and electronics on a silicon substrate using micromachining. The idea of using silicon for fabrication of mechanical structures has been around since 1980's [1] due to its outstanding mechanical properties in miniaturized systems. Thanks to the IC industry silicon is produced with very few defects at a low cost. A combination of silicon based microelectronics and micromachining allows the fabrication of devices that can gather and process information all in the same chip. This introduces powerful solutions within the automobile production, scientific applications and medical industries.

This Master Thesis was conducted at Nanofactory Instruments and at Solid State Electronics, MC2. Its aim is to design and produce a force sensor according to the specifications given by Nanofactory Instruments. The sensor will be a part in a specimen holder for Transmission Electron Microscope that is developed by Nanofactory Instruments for in situ atomic force microscopy and/or nanoindentation experiments.

### 1.1 Background

An in situ nanoindentation experiment has previously been done in an electron microscope [2]. The electron microscope provided real time images of the nanoindentation experiment. By performing an in situ analysis in a Transmission Electronic Microscope, TEM, the accuracy can be increased significantly, from a few nanometers in an electron microscope to angstroms in a TEM. It will also be possible to see phase transformations in the material caused by the force and thin native oxides.

The existing system at Nanofactory Instruments has the disadvantage that it is too large to be placed in a TEM. The sensor used is in fact an Atomic Force Microscopy, AFM, sensor with a silicon tip. It is desired to have an interchangeable tip in diamond to analyze a wider range of materials. The sensor cannot apply the higher force needed to do a nanoindentation test. The aim is therefore to produce a small force sensor that can measure higher forces with an integrated fixture for an interchangeable tip.

### 1.2 Methodology

The project was started with a literature survey to grasp the task. The goal was to look into the existing ways of design and manufacture a micromachined force sensor. This information was then used to assign a model and set up a process plan for manufacturing. The fabrication was performed and the sensors were evaluated using an initial test set up. The project outline is roughly divided in following parts:

- Literature survey
- Simulations and calculations
- Manufacturing
- Evaluation

Ink. t. Patent- och reg.verket

2004-01-26

Huvudförfattaren Kallgren

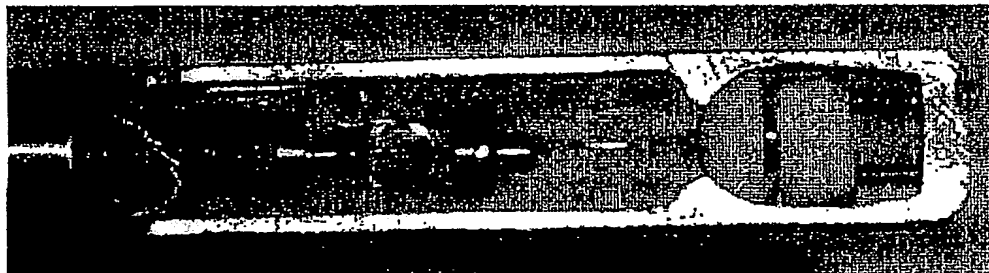
The report will follow this outline to provide insight to the reader for how the work was conducted.

### 1.3 Sensor Specification and Requirements

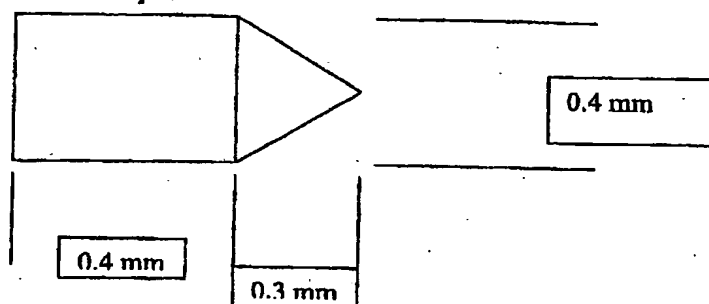
The force sensor will be placed in a specimen holder developed by Nanofactory Instruments, figure 1, for in situ measurements in a TEM, where AFM experiments or/and nanoindentation are conducted.

AFM is a method used to measure the topographic details of a sample surface. This can be compared to Scanning Tunneling Microscopy, STM, which has a higher resolution but can only analyze conducting materials. Nanoindentation analyzes the mechanical response of a surface or thin film by applying a known force through a sharp tip onto the sample. Of the criteria the sensor should fulfill the dimensions and the placement of the sensor are most critical. For optimal performance of the force sensor, it can be placed either in front of the sample or behind in the holder. The advantage of frontal placing is that the sensor will move instead of the sample during measurement. A disadvantage of this frontal arrangement is that noise will be induced and there will be less room to place read-out electronics close to the sensor. However if the sensor is placed behind the sample there will be more space for read-out electronics. Furthermore as the sample would move and the sensor will be still the noise level is reduced. Naturally the decision on sensor placement is dependent of its type. Appendix 1 contains CAD-drawings of the holder.

*Figure 1: TEM holder developed by Nanofactory Instruments for STM*



The sensor should be as general as possible as it is required to have an interchangeable tip. The tip used in the experiments has a diameter of 0.4 mm, figure 2, which is comparable to the sensor dimensions and this will limit the possibilities. Another restriction is that the tip will require a fixture to be placed in.

**Figure 2: The diamond tip**

In addition it is preferred to have multiple directions sensing as a force is being measured, thus giving a better overview of the examined sample. For summarized requirements see below and table 1.

#### Requirements:

Dimensions 2x2 mm maximum, preferably smaller

Integrated fixture for a diamond tip

Multiple directions sensing, preferably

The same design for nanoindenter and AFM sensor, preferably

**Table 1: Force ratings**

	Loading range	Absolute maximum load	Force resolution
Nanoindenter	0-100 $\mu\text{N}$	10 mN	0.1 $\mu\text{N}$
AFM	0-100 nN	10 $\mu\text{N}$	0.1 nN

## 2 Overview of Techniques Used in Combination with the Sensor

This chapter will explain the surrounding of the sensor and describe the kind of measurement required of it.

### 2.1 Transmission Electron Microscope

TEM functions as its optical counterparts apart from that TEM uses electrons for imaging. A stream of electrons is formed by a filament and is accelerated towards the specimen using a positive electrical potential. This stream is then confined and focused onto the sample in a specimen holder, using metal apertures and magnetic lenses. The electron monochromatic beam passes through the specimen, some electrons are scattered while the remainder are focused by the objective lens onto a phosphorescent screen or a photographic film to form an image. To make a TEM specimen, the sample is electropolished or etched by a Focused Ion Beam, FIB, to a thickness of 100 nm. The limited size of the sample makes the sample preparation very demanding.

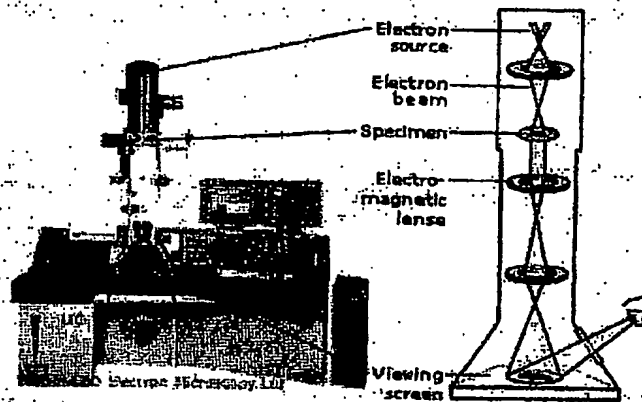
Ink t. Patent och reg.verket

2004-01-26

Huvudtaxen Kassar

There is a risk of the electron beam charging up for example a capacitive force sensor. If these charges are not transported away the relative capacitance change measurement can be disturbed. The stable temperature around the force sensor will do away of any temperature compensation.

*Figure 3: Transmission Electron Microscope, [3]*



## 2.2 Nanoindentation experiments

Indentation testing is a simple method that gives information on mechanical properties such as hardness and elastic modulus by pressing a tip into the sample. The method is originally from the Mohr's scale, in which materials that leave a permanent scratch on the materials are considered to be harder. Here, diamond has been assigned highest hardness value, 10.

Nanoindentation is an indentation test where the penetration scale is measured in nanometres instead of microns or millimetres as in more conventional hardness tests. The hardness and the elastic modulus are calculated from the resulting load-displacement curve when a force is applied to the material. The hardness is given by the first part of the curve, loading. When the force has reached its maximum, the contact area is measured and the hardness is given by equation 2.1. The slope of the load-displacement curve during the unloading phase provides a measure of elastic modulus. Equation 2.2 shows the elastic module for a multiple point indentation test [4].

Ink. t. Patent- och reg.verket

2004-01-26

Huvudfaxen Kassar

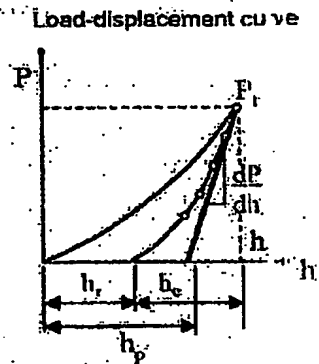
**Figure 4: Load-displacement curve of a multiple point indentation test [5]**

$$H = \frac{P_r}{A}$$

equation 2.1

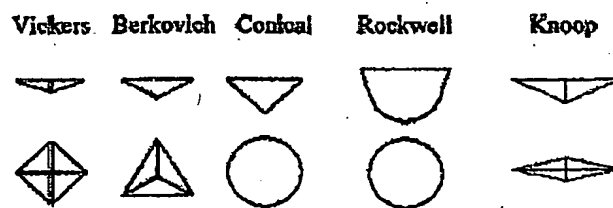
$$E^* = \frac{dP}{dh} \frac{\sqrt{\pi}}{\sqrt{A}} \frac{1}{2}$$

equation 2.2



The desire to perform nanoindentation grew from wanting to measure the hardness of thin films. The drawbacks of conventional indentation instruments is that they cannot apply the low force needed and even if it was possible the contact area cannot be decided with conventional methods. The scratch left is too small to be directly determined with for example an optical microscope. In nanoindentation the issue is avoided by measuring the depth of penetration with the sample positional system and comparing this to the known geometry of the indenter.

There are different kinds of indenter tips for different kind of measurements, see figure 5. Various tips are used depending on the material measured, the accuracy wanted and mathematical analysis method that is used to calculate the contact area [4].

**Figure 5: Various indenter tips [6]**

It is not only the hardness and the elastic modulus that is possible to measure with nanoindentation. The test can also determine the strain-hardening exponent, fracture toughness, viscoelastic properties etc.

### 2.3 Atomic Force Microscopy

Atomic force microscopy, AFM, is a part of the scanning probe microscopy family like STM. What distinguishes AFM from other scanning probe microscopes is that it can be used to

analyze insulators as well as conductors. A sharp tip on a cantilever is moved across the sample at a short distance. An interatomic force called van der Waal force will make the cantilever to bend or to deflect, depending on the distance between the sample and the tip. The force-distance function is presented in figure 7. The general idea is to keep the tip-sample separation constant through feedback while scanning the sample. The deflection of the cantilever is measured optically. Figure 6 gives a general picture of how an AFM works.

Figure 6: AFM, [7]

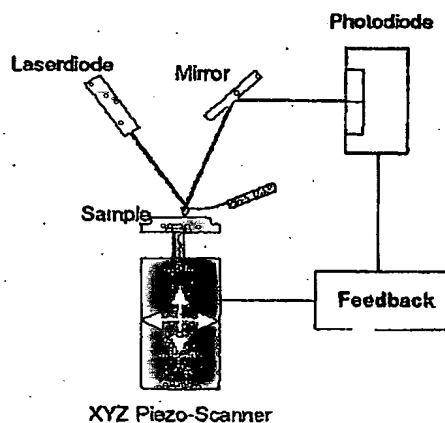
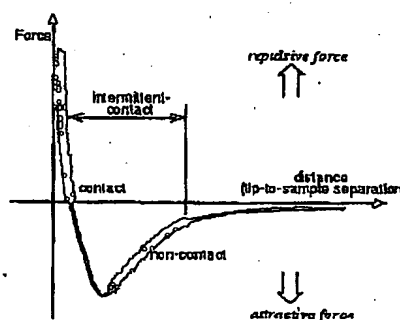


Figure 7: Force-distance function, [8]



The force-distance dependence is not linear and there are three modes to work in where the function is relatively stable. The operation modes are: contact mode, temporary contact mode (tapping mode) and non-contact mode. In contact mode the cantilever is held less than a few angstroms from the sample surface and the inter atomic force is repulsive. In non-contact mode the cantilever is held on the order of tens to hundreds of angstroms from the sample and the force is attractive. The tapping mode is usually preferred since an accurate measurement can be done with minimal surface alteration.

A drawback with this system is the size and weight of the optical system. In this application space is a major issue and there is no room for a large optical system. To avoid this other read-out solutions such as piezoresistive and capacitive sensing will be investigated in this work.

### 3 Force Measurements

Depending on the application there are several ways of measuring force; ie by resonance frequency, bending moment, deflection or torsion. One of the most common ways to measure force is to use an elastic element on which a force is applied and the value of the force is decided from the bending moment, torsion moment or the deflection it causes. This introduces different electrical and mechanical measurement systems. There are several measurement

systems that can be used for force sensing, the most common ones and the ones interesting for this project are:

- Capacitive measurement
- Piezoelectric
- Piezoresistiv
- Resonance

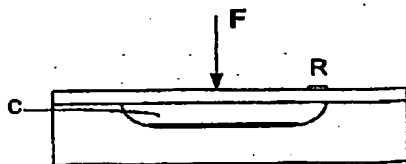
Two of the methods could directly be excluded for use in this project due to consistency problems. A resonant read out would be too difficult to integrate with the diamond tip on the sensor and a piezoelectric solution is too hard to implement since with the chosen silicon this is not a piezoelectric material. Even if it is possible to deposit a piezoelectric material on silicon this is a complicated process that is not available at the MC2 laboratory at this stage of writing. Therefore the scope of this master thesis is narrowed to investigated the capacitance and the piezoresistive read-out methods.

### 3.1 Capacitive Sensing

Capacitive measuring is widely used in many different applications. The method is simple in theory and is relatively easy to realize. The method has several advantages such as good accuracy, low temperature dependence and that it is convenient to manufacture with microfabrication. Figure 8 contains a schematic picture of a capacitive force sensor with a membrane as one of the capacitor plates. When the force is applied the membrane deflects and the capacitance changes.

The major drawback of miniaturizing a capacitive sensor is that the output signal is highly dependent on the plate areas, which yields an output in the same order as the noise for many micromachined devices. The parasitic and stray capacitances complicate the measurement. The electronic setup has to be very close to the sensor to avoid as much of the parasitic effects as possible. This is something that complicates this project where space is a critical parameter.

*Figure 8: Schematic view of a micromachined force sensor with a membrane*



### 3.2 Piezoresistiv Sensing

Piezoresistivity is a material property where the bulk resistivity is affected by the mechanical stress applied to the material. The high piezoresistivity and the good mechanical properties of silicon makes it well suited for conversion of mechanical deformation into an electrical signal. The piezoresistive element is in micromechanical terms high-doped monocrystalline silicon.

As seen in figure 8 the piezoresistive element is placed where the maximum strain is to get a high output as possible.

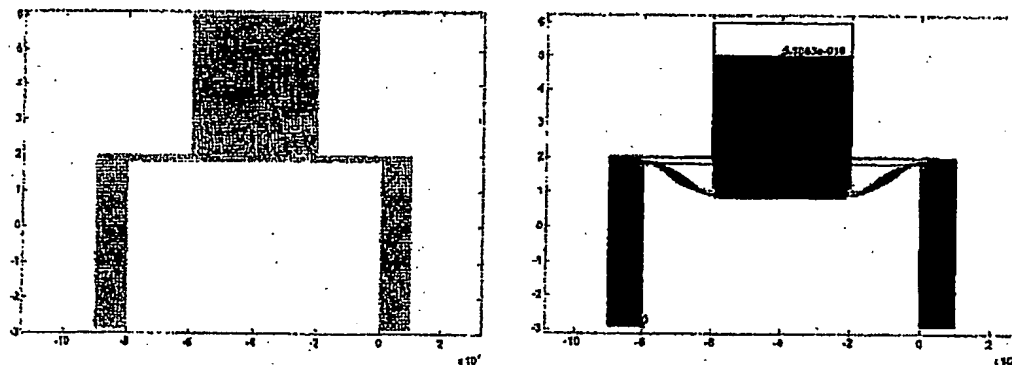
Using the piezoresistive property of silicon has the advantage that the read-out signal is less sensitive to the electromagnetic interference from the environment. This is an important quality since the sensor will operate in a TEM. The disadvantages are high temperature dependence and a more complicated fabrication. In this case an integrated fixture affects the sensitivity of the sensor. There can also be problems with high doping a small area with existing equipment in the MC2 clean room.

## 4 Design and Calculation

### 4.1 Initial Nanoindenter Sensor Simulation

To investigate which model to use to design this sensor analytical calculations and FEMLAB simulations were done. A first model was chosen, the model consists of a membrane holding a stiff body, see figures 9. The stiff body represents the diamond tip in its fixture, the fixture is assumed to be 0.1 mm thick ring. A force of 0.1  $\mu$ N was applied to the stiff body on the membrane and the displacement was simulated. The displacement is important since it decides how large the relative capacitance change will be, a displacement as large as possible is required.

Figure 9: The first model simulated in FEMLAB



### 4.1.2 Capacitive Model Simulation

In the simulations the membrane thickness was altered. It is known from microfabrication methods that it is possible to get about 20  $\mu$ m thin membrane using only a time stop. The variation was therefore in that range. The capacitance was calculated with equation 4.1 where the  $d$ , the gap, is assumed to be 2  $\mu$ m and the dielectric air. The area,  $A$ , is 0.8x0.8mm<sup>2</sup>.

$$C = \frac{\epsilon \cdot A}{d}$$

equation 4.1

The simulations quickly showed that the deflection was not enough it needs to be several magnitudes higher. Table 2 presents the simulation results. A search for a commercial capacitive read-out circuit showed that 0.5 fF is the lower limit for what can be measured off-chip. In this case the thickness has to be even thinner than 2  $\mu\text{m}$  to get an output close to that. The sensors would then be very fragile and it would not be possible to transport without breaking the membrane. The programs used for calculations are found in appendix 4.

Table 2: Capacitive model simulation result

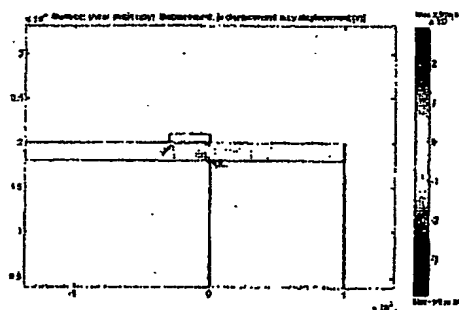
Membrane Thickness [ $\mu\text{m}$ ]	Displacement [m]	Relative Capacitance change [F]
30	2.0e-16	1.81e-22
20	5.5e-16	4.98e-22
10	3.6e-15	3.26e-21
5	2.7e-14	2.45e-20
2	4.0e-13	3.63e-19

Since the simplest model was so far away from what is required for this purpose it was reasonable to conclude that there probably are no commercial sensor that can fulfill the specifications. The design has to be made especially for this work, and the best option to achieve this is to fabricate it within the scope of a master thesis.

#### 4.1.3 Piezoresistive Model Simulation

An alternative piezoresistive solution was also investigated. A piezoresistive element in highly doped silicon was placed where the strain was highest, see figure 10, when a force of 0.1  $\mu\text{N}$  is applied according to figure 9. The changes in the piezoresistive element was observed and calculated. Equation 4.2 shows the relative resistance change due to the strain in the material.

Figure 10: Piezoresistive model



$$\frac{\Delta R}{R} = (1 + 2 \cdot \nu + \pi \cdot E) \cdot \epsilon$$

equation 4.2 [9]

Where  $\nu$  is the Poisson ratio,  $\pi$  is the piezoresistive coefficient of the material,  $E$  Young's modulus for the material and  $\epsilon$  is the strain.

Table 3: Piezoresistive model simulation result

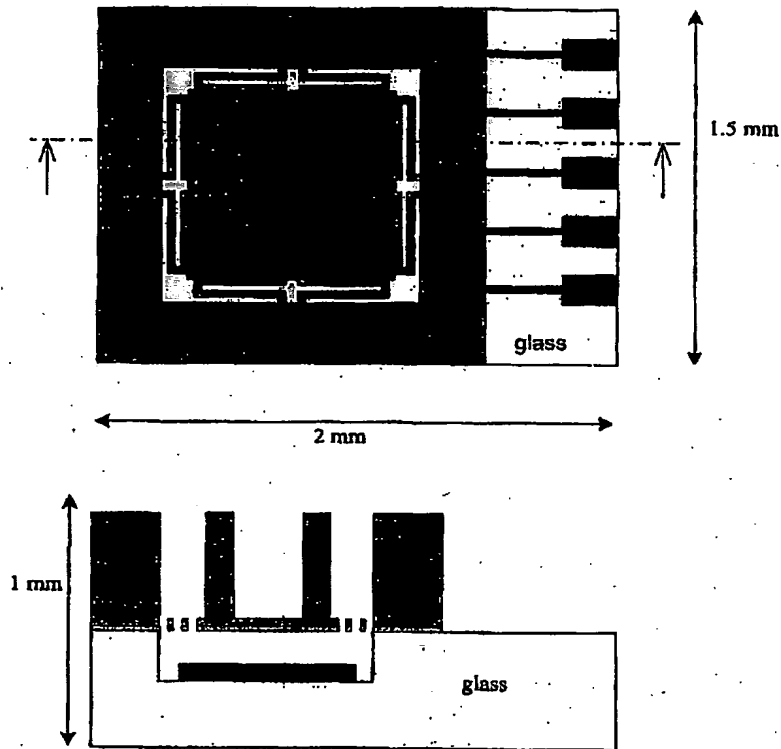
Membrane thickness [ $\mu\text{m}$ ]	Strain, $\epsilon$	Resistance change [ $\Omega$ ]
30	9.4e-14	1.7e-11
20	2.9e-13	5.2e-11
10	7.7e-13	1.4e-10
5	5.9e-12	1.1e-9

As the simulation results show in table 3 the resistance change is marginal for the applied force. The holder clearly makes the structure so stiff that decreasing the thickness of the membrane is not enough to get a higher output. Additional complication concerns the manufacturing of a piezoresistive sensor, the diamond tip and its fixture will make it hard to place the piezoresistive elements on the top of the sensor. The elements will have to be placed underneath the structure and this adds several process steps.

Based on these reflections it was decided to continue on a capacitive sensor design. The piezoresistive sensing shows very low output levels and when it comes to measuring low output levels it is easier to measure capacitance. Manufacturing a capacitive sensor will also be more convenient since there are established fabrication methods in MC2 laboratory.

#### 4.1.2 Final Nanoindenter Sensor Design

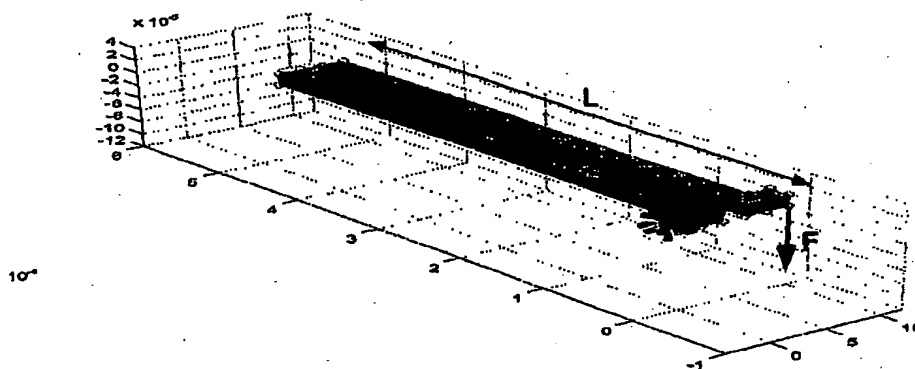
The integrated fixture for the diamond tip limits the design; the tip will add the flexibility that is desired for interchangeable tips but it also induces new complications during fabrication. As concluded from previous calculations the fixture does not leave much room for a membrane, therefore that what is left of the membrane must be very weak. Using regular silicon 6-inch wafer a thickness of 20  $\mu\text{m}$  is the lower limit where it is possible to make the membrane without risking etch away what is left of it. One way of weakening the structure is to use springs. So instead of membrane springs were used to attach the fixture to the wall. The springs are evenly placed around the tip holder; the structure has to be symmetrical to measure the direction of the force. To have multiple directions sensing the aluminium plate can be divided in four parts, see figure 10. The relative capacitance change will give a measure of the force direction. The gap between the silicon and the plate on the glass is a critical parameter, it should be as small as possible to have as high capacitance as possible. The highest deflection of the upper plate will determine the gap. The final design is seen below in figure 10. To decide the dimensions FEMLAB simulation was done.

**Figure 10: The final sensor design**

To simulate the design an approximate model is needed, it would require too much computer power to simulate the actual design. In the model the approximation is to consider the fixture and the area around it a stiff body. This approximation will result in an underestimated displacement. The approximation error should be relatively small. It will be enough to simulate only one of the springs with  $1/8$  of the total force applied at one end. The spring's displacement is simulated and with that information the relative capacitance and resonance frequency is calculated.

Different spring height, length and width were considered to find the optimal dimensions. The height can as minimum be  $20\text{ }\mu\text{m}$  due to processing limitation, simulated dimensions will therefore be in that range. The model was drawn in FEMLAB and the material set to silicon. A force of  $0.1\text{ }\mu\text{N}/8$  was applied to one end of the spring as seen in figure 11 and the other end of the spring was fixed.

Figure 11: Spring model simulated in FEMLAB



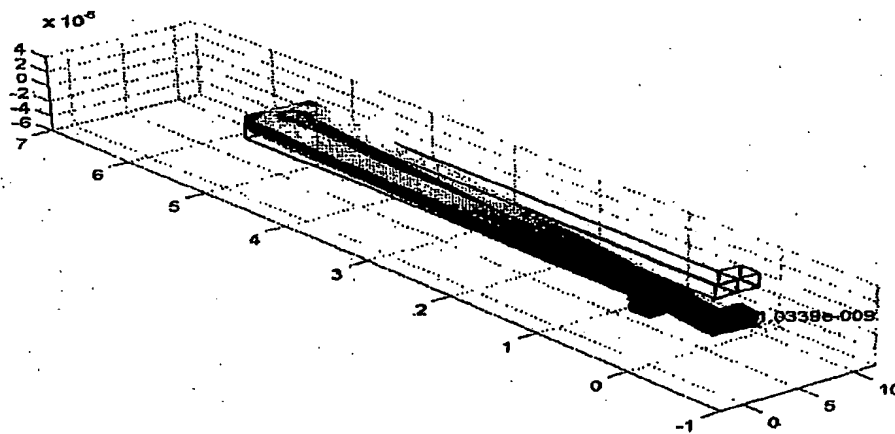
The general behavior of the spring is expressed in equation 4.3. The equation applies in fact in the case of a suspended beam but can serve as a rough approximate calculation for this case. The displacement is:

$$\delta = \frac{F \cdot l^3}{3 \cdot E \cdot I} \quad \text{equation 4.3}$$

$$I = \frac{b \cdot h^3}{12} \quad \text{equation 4.4}$$

Where  $b$  is the width and  $h$  the height of the spring.

The height of the springs affects the displacement most as seen in equation 4.3 and 4.4 and in FEMLAB simulations. Other parameters such as width is also affected by the spring thickness, it is not desirable to have a width much smaller than the height since it could result in torsion and unsymmetrical behavior of the sensor. The height is already decided to 20  $\mu\text{m}$  so it is suitable to choose the width to 20  $\mu\text{m}$  as well. The length should be set to as long as possible to get higher displacement. Two springs has to be placed on each side of the tip holder therefore the maximum length is 500  $\mu\text{m}$ . These parameters, length and width, will not be varied in further simulations. Using these dimensions the displacement for the resolution force, 0.1  $\mu\text{N}$ , was about 1 nm, figure 12. The capacitance when no force is applied is calculated with equation 4.1 with  $A$ , plate areas, as  $0.8 \times 0.8 \text{ mm}^2$  and  $d$  as 2  $\mu\text{m}$ . The resulting capacitance is 2.8 pF. Simulation results for different spring heights are found in table 4. The programs used to calculate the parameters in found in appendix 4.

Figure 12: Simulation result,  $h=20\mu\text{m}$   $b=20\mu\text{m}$   $l=500\mu\text{m}$ 

To test different designs in the process an extra bend is added to some of the component manufactured. Other parameters that are varied in the processing of the sensor are the spring width and the inner fixture diameter.

Table 4: Summarized results from simulations on spring when applying the resolution force:

Spring height [ $\mu\text{m}$ ]	Deflection [nm]	Relative capacitance change [fF]	Resonance frequency [kHz]	Spring constant [N/m]
15	2.42	2.2	1.7	41
20	1.03	1.4	2.6	98
30	0.83	0.75	2.9	120

As seen in table 4 the sensitivity of the sensor is  $1.4 \text{ fF}/0.1 \mu\text{N}$  for spring thickness of  $20 \mu\text{m}$ . A search in available commercial capacitance read-out circuits shows that this sensitivity is within the range of what is possible to measure. However it is important to remember that even though this design will have a measurable output there is still reason to plan surrounding electrical equipment like connection cables with care.

## 4.2 AFM Simulations

As mentioned in chapter 1.3 it is preferred to use the same design for the nanoindentation and the AFM sensor. The force range the AFM sensor is specified for is 1000 times smaller than the nanoindentation force range. One way to make the proposed design in figure 10 more sensitive is to decrease the spring thickness even more. From manufacturing point of view it is possible to make as thin springs as  $5 \mu\text{m}$  if Silicon On Insulator, SOI, wafers are used. The

structure would be very fragile and needs to be handled with extreme care. The cost of each individual sensor will increase due to the higher cost of SOI wafers.

Simulations were done by applying one eighth of the resolution force (0.1 nN) for the AFM sensor on one end of the spring and fix the other end, see figure 11. The length of the spring was set to same dimension (500  $\mu\text{m}$ ) as in the nanoindenter sensor simulation and the width was decreased to 10  $\mu\text{m}$  to make the design even more sensitive. Other than that the simulations were conducted in the same manner as in chapter 4.1.2. The results are seen in table 5.

**Table 5: Results from simulations on structure when applying 0.1 nN**

Spring height [ $\mu\text{m}$ ]	Deflection [m]	Relative capacitance change [F]
15	3.1e-12	4.4e-18
10	9.8e-12	1.4e-17
5	7.7e-11	1.1e-16

The relative capacitance change is too low for this application where an on-chip read-out circuit is not available.

There are some ideas for other AFM sensor designs if the diamond tip can be compromised with. A differential capacitive sensor using force balance is proposed by Joyce and Houston [10], something similar to this design would be suitable also in this case. The differential capacitance measurement would eliminate surrounding effects on the sensor and increase the sensitivity.

### 4.3 Motivation of Chosen Design

When considering the information from literature studies and simulations it was decided to continue with the nanoindenter design that is proposed in figure 10. The design fulfils all the requirements and it is relatively clear how it can be manufactured. One problem regarding the read-out has a possible solution. A highly sensitive small circuit (1.6x1.9mm) has been found. The circuit is small enough to fit in the specimen holder and can therefore be placed very close to the sensor. The accuracy of this circuit is 0.5 fF, which is well enough to measure the force sensor's read-out capacitances.

To fabricate an AFM sensor within this diploma work will not be done since the diamond tip that is required for the nanoindentation experiments inhibits the use of the same design for an AFM and nanoindenter sensor at this stage. Fabricating two different sensors is not realistic in the amount of time available in a master thesis.

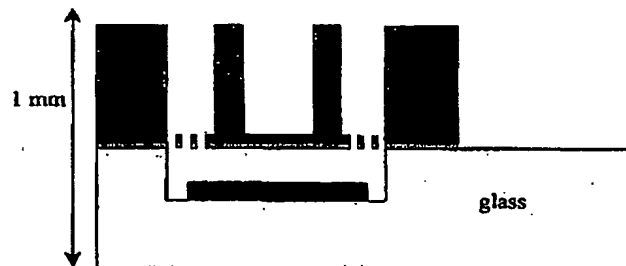
## 5 Manufacturing

The fabrication was performed in MC2:s clean room at Chalmers. The main process steps are mask alignment, RIE Reactive Ion Etch, aluminum evaporation and different kind of wet etching. These and some more steps will be explained in this chapter. There is a detailed plan of how the processing was conducted, containing the results of the processing in appendix 5

## 5.1 Device structure

The force sensor consists mainly of two parts, a silicon part where the springs are defined and one part in glass where the electrodes are defined. Glass is chosen for the bottom part due to its high dielectric property. The silicon and the glass are processed separately until the last step, which is to anodically bond the silicon to the glass.

*Figure 13: A cross section of the force sensor*



A double-sided lithography is needed to process the silicon in the shape required. First the springs are etched from the backside and the front is etched until the springs can be seen. At this stage the wafer is very fragile and needs to be handled with great care.

## 5.2 Mask design

The patterns needed for manufacturing were made in Cadence layout program. Different layers are used to define the masks. To fabricate the structure a number of masks are needed, the number should however be kept as low as possible. This not only because of the cost of each mask, but also of consideration to the resulting process, which intends to be simpler with fewer masks. Manufacturing of masks was done at Uppsala University, since the machine needed was out of order at Chalmers.

The following masks were made to manufacture the force sensor.

- Mask one:** Patterns for an oxide mask for etching of the holder and wall structure. The oxide mask is needed for the deep dry etch.
- Mask two:** Pattern to etch the springs from the backside. This mask determines the width of the beams. The saw marks are also done in this mask.
- Mask three:** This mask defines the glass cavity and the electrode trenches. There are two variations, one with recesses for two electrodes and one with recesses for four electrodes.
- Mask four:** The mask determines the metal plate and the pads. The variations are the same as in mask three, one where two electrodes are deposited and one where four electrodes are deposited.

During processing it was noticed that the oxide mask was not resistant enough so a layer of photoresist was put on the oxide mask. Mask one is therefore used twice in this process. The

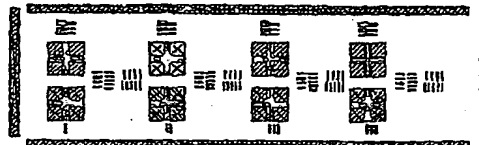
masks contain variations to tests different designs and to ensure some safe designs. All the mask variations are seen in appendix 2.

### 5.2.1 Alignment marks

Three alignment marks are needed to fabricate this structure, one to align the holder pattern to the spring pattern, one to align the glass recesses to the metal electrodes and one to bond the glass wafer to the silicon wafer. To minimize the risk of losing alignment marks during processing an extra pair of alignment marks were placed vertically. Alignment marks for 3-inch wafers were also drawn in the mask so that if any problems would raise with 6 inch processing it would be possible to use 3-inch wafers.

The numbers beneath every alignment mark, in figure 14, show the order in which the wafers are aligned. These marks are needed to avoid aligning with the wrong alignment mark. Due to the use of double-sided lithography in the processing the alignment mark groups are placed 8.5 cm apart to fit the Karl Suss MA6 aligner.

Figure 14: Alignment marks



For a rough alignment a flat edge marking is used. Aligning with the flat edge is not an accurate method but it gives a satisfactory initial alignment. It is also a convenient way of knowing which way is up on the mask just by looking at it.

Figure 15: Flat edge mark



Two recesses were done at each end of the flat edge mark; these are made to minimize the rotation error. The flat edge mark is done in every layer used.

### 5.3 Performed process steps

The following chapter explains the different process steps that were utilized. It provides background for understanding micromachining better and for how the processing was conducted. See appendix 5 for more detailed information concerning the processing.

M. J. P. P. P. P. P.

2004-01-21

M. J. P. P. P. P. P.

### 5.3.1 Oxidation

The deep etching step requires an oxide mask, oxide has the high enough selectivity to silicon in dry etching. The selectivity is 200:1 or higher, that is when 200  $\mu\text{m}$  silicon is etched 1  $\mu\text{m}$  of the oxide is etched.

The oxide ( $\text{SiO}_2$ ) can be "put" on the silicon in different ways, it can be grown or deposited. Since the oxide will be used as a mask a high quality is necessary. Grown oxide is known to have better quality than deposited oxide, so the oxide was grown using wet oxidation. It is also possible to use dry oxidation to grow the oxide as it even has better quality than oxide grown in wet environment, but it would take several days to grow 2  $\mu\text{m}$  oxide. The difference between wet and dry oxidation is that in wet oxidation water vapor is used to grow the oxide and in dry oxidation oxygen gas.

### 5.3.2 Boron Doping

Boron has a diffusion coefficient of about  $10\text{--}12 \text{ cm}^2/\text{s}$  at  $1150^\circ\text{C}$  [11]. It has a high solid solubility which makes it very suitable as dopant. The doping process will consume some silicon according to equation 5.1:

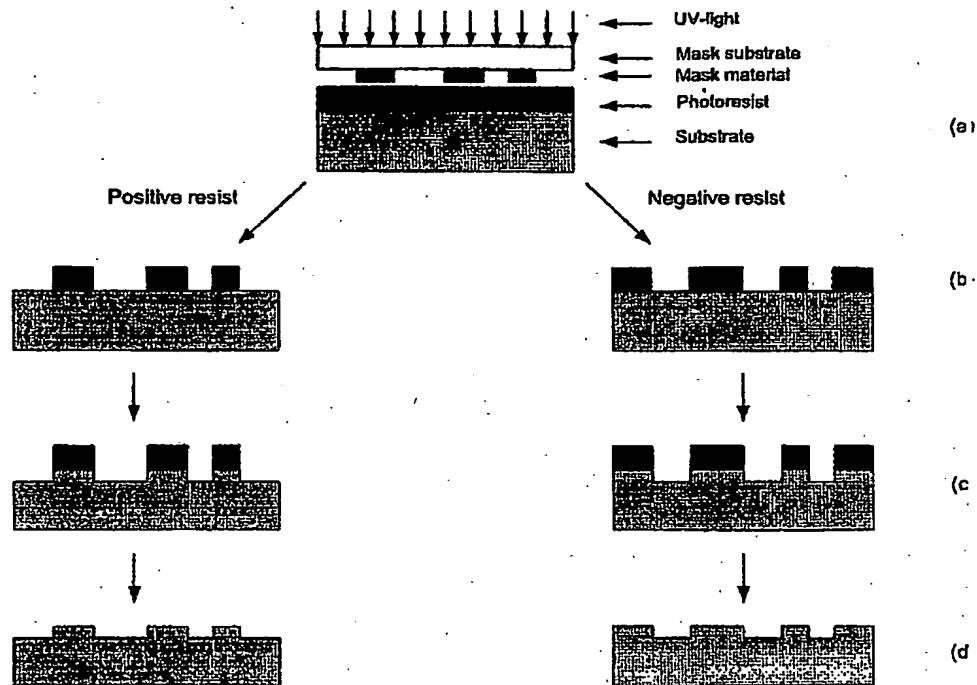


The silicon wafers are placed in a boat facing boron wafers; the boat is then inserted into an oven with inert environment where it is heated to  $1040^\circ\text{C}$ . The temperature is  $1040^\circ\text{C}$  for 30 minutes and then the temperature is gradually lowered. After this step a boron skin has been formed on the silicon wafers. This boron skin, a form of boron oxide, causes dark brown stains that are electrically insulating. The boron skin is very hard to remove in any acid but if it is oxidized wet a form of borosilicate is formed which can be removed with hydrofluoric acid.

There were some mistakes done when doping the silicon wafers, the first mistake was the time the wafers were doped. It should have been 1 hour instead of 30 minutes to achieve the doping goal. The second mistake was during the wet oxidation step, if the temperature is too high the dopants are driven a bit inside the silicon wafers. This can be desirable in some cases, but not in this process. The set temperature was  $1000^\circ\text{C}$ ; it should have been  $750^\circ\text{C}$ . The measured doping is 40  $\text{ohm}/\text{square}$ ; the expected doping was 12  $\text{ohm}/\text{square}$ . This was not investigated further since the doping level is high enough to get an ohmic contact between silicon and aluminum.

### 7.3.3 Lithography

The most common lithographic technique is Ultra Violet (UV) photolithography. It is used to transfer patterns using ultra violet light. A schematic picture is given in figure 16. The pattern is defined with a reflecting material, usually chrome, on a transparent material such as quartz. The mask is then exposed to UV-light that is reflected on the areas where there is chromium and passed on to a radiation sensitive polymer film through the openings.

**Figure 16: Pattern transfer with different kind of resist**

The radiation sensitive material is called photoresist, usually only resist. It is a polymer and can be of two types, positive or negative. UV-light has opposite effects on positive and negative resist: when exposed to UV-light and put in a developer the exposed parts of the positive resist is dissolved and vice versa for negative resist, see figure 16 (b). In figure 16 (a) there is a small gap between the mask and the wafer, this is called proximity mode. It is also possible to work in contact mode, the mask is then in contact with the wafer. Contact mode has a higher resolution but it is rough to the mask. There is a risk of resist release from wafer, as the silicon is pressed harder to the mask.

### 5.3.4 Dry etching

There are different ways of etching silicon, wet or dry, isotropic or anisotropic. The force sensor fabricated in this project needs well-defined straight walls. The best way to achieve this is to use dry etch, which will give an anisotropic etch. The dry etch method used is called DRIE-Deep Reactive Ion Etching. ICP-Inductive Coupled Plasma was used to manufacture the force sensor. The name ICP refers to how the plasma is created, here it is by an inductor. There are a number of gases which can be used to etch materials such as silicon, oxide or silicon nitride.  $\text{SF}_6$  is and some oxygen is used to etch silicon.  $\text{SF}_6$  is an isotropic silicon etchant the anisotropic etch behavior is achieved by using a cycled process containing two

steps, first step is to deposit a thin layer of polymer and the second step is to etch the silicon with  $\text{SF}_6$  plasma. This is called the Bosch process.

The etch rate is highly dependent of the pattern, it is important to be aware of this when designing the masks. Open areas will etch faster than smaller ones and edges are etched faster than the center. Also the outer part of a wafer is etched faster than the inner parts, this is something which will affect which components that will survive the processing in this project. Standards wafers are used, this means that there is no (material) etch stop such as buried oxide. This limits the process to a time stopped dry etch. Therefore some of the components will break during this step making it necessary to decide to keep the outer or the inner components. Another complication that was discovered when dry etching silicon was that the left side of the wafer etched faster than the right side. The person responsible for the tool had no explanation for what could cause this. Appendix 5 contains more details about the dry etch steps.

### 5.3.5 Glass etch

To etch the bottom glass a wet isotropic etch was used. The acid used, HF, is very aggressive and the mask material should therefore be of chromium or gold. Unfortunately this is not possible to deposit a 6-inch wafer with either of the materials in MC2 clean room. Experiments were done using only photoresist. The thin photoresist did not last the 4 minutes needed to etch 3  $\mu\text{m}$ . A higher concentration of HF was needed. Thin photoresist was not tried in higher concentration HF, it would not last thick photoresist is more resistant. The glass wafer was patterned with thick photoresist and baked for 1 hour in 120  $^{\circ}\text{C}$ . To minimize the time needed for etching 50% HF was used. The use of 50% HF is avoided due to its aggressive nature, but here it was no other solution. The glass needs to be etched for 23 s to achieve 3  $\mu\text{m}$ . The accuracy of the etching was about 10%, this can be done better if a lower concentration of HF can be used.

### 5.3.6 Metal deposition

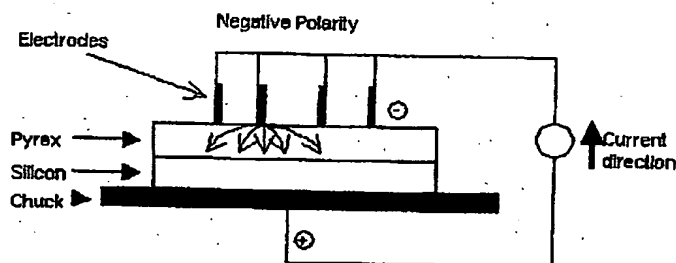
Aluminum was used as electrodes and as a capacitance metal plate on the bottom glass, aluminum since that is the only metal that can be deposited on a 6-inch wafer. It would have been better to use gold, gold is an inert element which would not react with the environment. Aluminum rapidly forms an insulating oxide, which is hard to get through without some force. There are two ways of depositing metals, by sputtering or by evaporation. In this project evaporation was used. The metal is heated above the vapour temperature in a low-pressure atmosphere, the metal will then evaporate and deposit the wafer. The wafers are rotated in the chamber to get more uniformity. Evaporation of metal does not have good step coverage, so if deep trenches are to be deposited by a metal, sputtering should be used.

### 5.3.7 Anodic bonding

Anodic bonding refers to bonding between an electrically conducting plate, such as silicon and a glass wafer that becomes conductive when heated. A negative voltage is applied to the silicon and a positive voltage to the glass, the voltage can from 200 to 1000 V depending on the thickness of the glass and the temperature. The temperature range is 180  $^{\circ}\text{C}$  - 500  $^{\circ}\text{C}$ . The

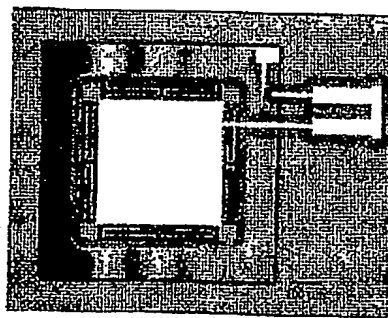
electric field will be concentrated to a thin depletion layer in the glass and in the gap between the wafers. If the wafers are smooth enough the electrostatic pressure is enough to join the wafers. The combination of high temperature and high field causes chemical bonds to form between the silicon wafer and the glass substrate [12]. Glass substrates with thermal expansion coefficient to silicon are used to minimize thermal stress. The glass types used for anodic bonding are part of the borosilicate crown glass family. Pyrex is the most frequently used glass due to its advantageous properties such as low thermal expansion coefficient of expansion and the fact that it is inexpensive [13]. Schott Borofloat, the glass used in this project, is another member of the borosilicate crown glass family. Borofloat has similar properties to Pyrex; the difference lies in the production method.

Figure 17: Anodic bonding setup



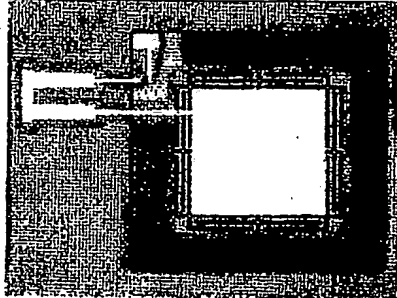
The anodic bonding step was complicated by the thickness of the press contact. The deposited thickness of the aluminum was about  $1\text{ }\mu\text{m}$ ; due to this thickness a large area around the press contacts was not bonded. A few edge components were partially bonded, see figure 18.

Figure 18: A partially bonded device

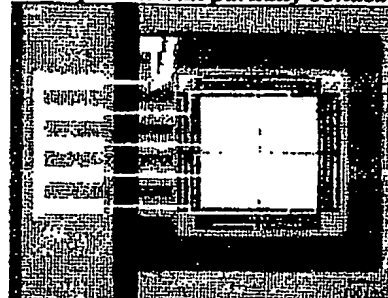


The aluminum was thinned to  $0.45\text{ }\mu\text{m}$  and the voltage was increased to get better bonding. The combination worked very well and the bonding was successful this time. However the springs on some devices were also bonded to the glass. This can easily be avoided next time by using a lower voltage. Figure 19 (a-b) shows components from the successful attempt.

**Figure 19 (a)**  
**A successful bonded component**



**Figure 19 (b)**  
**A component with partially bonded springs**



The electrodes are interconnected to have the same voltage on the aluminum plate as on the silicon. This will avoid bonding the plates. It was later understood that this was not really necessary, the aluminum it self is enough to inhibit wafer bonding on that area. For more detailed information on the anodic bonding attempts see appendix 3.

#### 5.4 Process Comments

The process plan was altered several times during processing, due to different kind of complications. In this section changes to the process plan will be discussed. Some helpful tricks are also documented here.

##### 5.4.1 Oxide mask enhancement

To have one wafer at the end that will give working component, 10 silicon wafers and 6 Borofloat glass wafers were processed in parallel. The 2  $\mu\text{m}$  grown oxide was not enough as mask and it was enhanced with 8  $\mu\text{m}$  thick resist. See appendix 6 for further details such as resulting etch time. The alignment in this step was hard to get accurate, the oxide mask was like a shadow and the accuracy was hard to decide during alignment.

##### 5.4.2 Dry etch problems

The alignment marks were etched off during the deep etch step, as mentioned before smaller areas etch slower than open. To protect the alignment mark for the next step, anodic bonding, some aluminium foil was put on the mask covering the alignment mark groups. This worked very well except that it was hard to put the foil so that it only covered the alignment marks and not any components.

The cooling was not even throughout the wafer and high temperature increased the etch rate so much that many fixtures were etched off. Figure 20 shows a cross section of an etched away diamond fixture.

**Figure 20: Etched away diamond fixture**



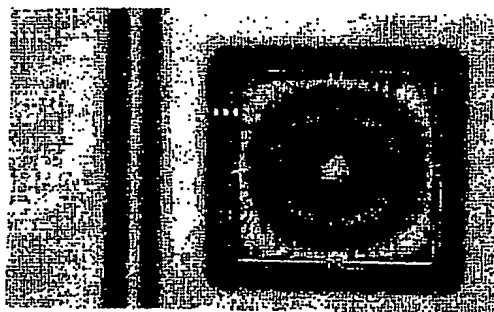
### 5.4.3 Glass processing

The chuck used complicated the lithography of the glass wafer. The glass itself is transparent to UV-light but the chuck is made of metal, which reflects light. The metal chuck has two large holes that are used in backside lithography; this makes the reflection of the light uneven over the wafer. This did not affect any components since the hole did not cover any. If this step is critical a metal should be deposited on the glass to achieve an even reflection or use a glass chuck.

## 6 Evaluation

There were about 1000 sensors on the wafer produced, of these 1000 about 150 seemed to be functional and has been sawn into single devices. Figure 21 contains a picture of a fabricated sensor seen from above. About one third of the devices had their tip holders intact, the rest appear to be functional except for lacking the integrated fixture. These sensors will be used for initial evaluation.

**Figure 21: The manufactured sensor**



Capacitance-Voltage (CV) measurement was used to examine the components. The first concern was to determine whether the springs in the system are clearly free and the capacitive plate actually moving and the second to study the relative capacitance changes.

## 6.1 CV-measurements

The concept of the measurements is to put a DC voltage across the silicon and the aluminum on the glass. The voltage will induce an attractive force on the plates forcing them closer. When the absolute value of the voltage is increased and the distance between the plates decreased the capacitance is expected to follow that according to equation 6.1.

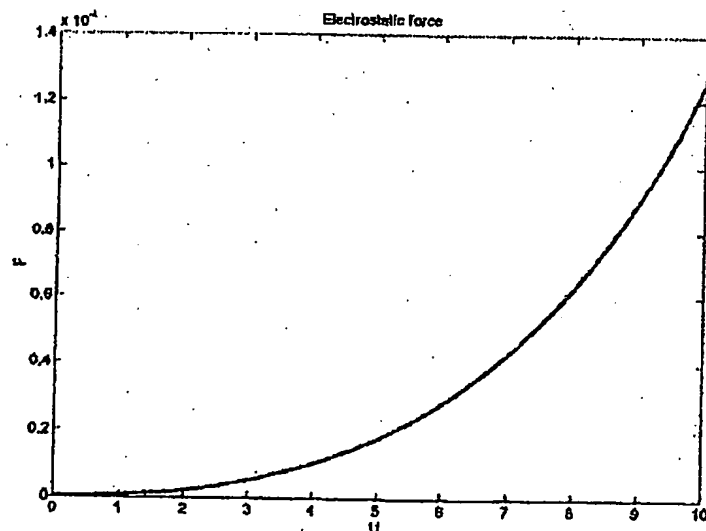
$$C = \frac{\epsilon \cdot A}{d} \quad \text{equation 6.1}$$

The sensor specifications give that the capacitance should vary when forces in the range of 0.1  $\mu\text{N}$ –0.1 mN is applied. Equation 6.2 shows the relation between the electrostatic force and the applied voltage.

$$F = \frac{\epsilon \cdot A \cdot U^2}{2 \cdot d^2} \quad \text{equation 6.2}$$

To roughly calculate the force applied with respect to the changing distance of the plates the simulated values of the deflection is used. Figure 22 shows that a voltage variation of 100 V should be more than enough to get the total capacitance variation.

**Figure 22: Electrostatic force vs. applied voltage**

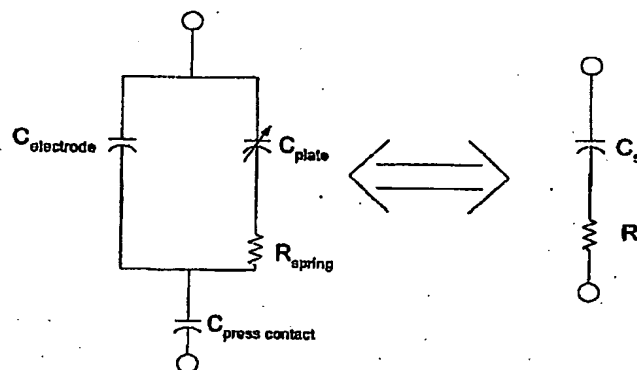


An electrical circuit scheme of the force sensor shows the capacitances in the sensor and helps us to choose the right model for the measurements. The equivalent circuit scheme is seen in figure 23. A comparison with the sensor it is obvious that the capacitance and resistance  $r$  series model should be chosen. The other choice is a capacitance in parallel with a resistor.

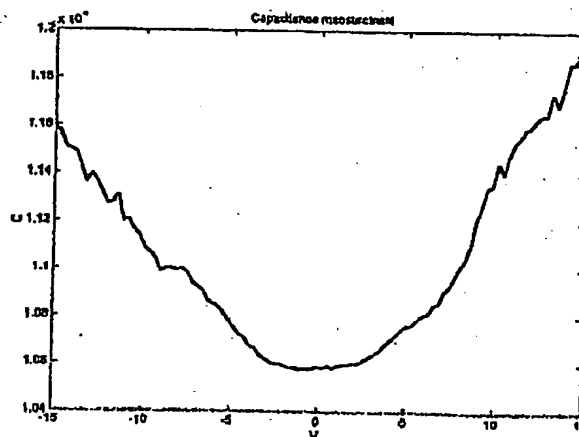
Int. t. Patent sch. reg.

2004-01-21

Revolutio. no. 115.

**Figure 23: The equivalent circuit**

Several measurements were done on about 15 sensors and on several of them exposed a force dependent capacitance change. The voltage was varied from negative to positive to examine the capacitance values around 0 V. The capacitance curve looks almost as expected, the capacitance begins with high value to decrease with the absolute value of the voltage and reaches a minimum value a 0 V to increase again when the voltage is increased, see figure 24. This clearly indicates a variable capacitance controlled by the electrostatic force.

**Figure 24: A typical result from CV-measurements**

The capacitance values do however not agree with the simulated values. The capacitance here are about 1 nF and the calculations predicted that they should vary around 2.26 pF<sup>5</sup>. A closer look on the measured curve shows that there are two different slopes. The slope of the curve in region 0-3 V is much lower than the slope in 3-15 V. A calculation on several sensor measurements shows that the slope in the range of 0-3 V is about 0.8 pF/V and this is closer

<sup>5</sup> The distance between the plates are now 2.5  $\mu\text{m}$  due the thinned aluminium

to the expected values. This can be an indication of two super positioned phenomena being measured. There is also a possibility of something other than air is acting as the dielectric in the sensor. During the processing the sensors are washed in different chemical for cleaning and some of these chemicals might still be inside the sensor. Treating the sensors in a vacuum oven can solve this problem.

In addition to the CV-evaluation successful tests has been done by Nanofactory Instruments to place a wire/tip in the integrated fixture without breaking the sensor.

There is unfortunately no more time to continue the evaluation within the master thesis, these issues has to be investigated further in future work. Future testing can be conducted with an evaluation board and a capacitance read-out circuit with an accuracy of 0.5 fF ordered from SmartTec in Holland.

## 7 Conclusions

A nanoindenter force sensor with an integrated fixture for a diamond tip has been designed and fabricated. Initial measurements confirm that the sensor has a force dependent capacitance change when a force within the specified range is applied. The capacitance values measured do however not completely confirm the theoretical calculations and simulations. Further evaluation is needed.

A critical part in this processing was the deep dry etch to shape the integrated fixture and free the springs. This step can be improved by using Silicon On Insulator, SOI, wafers. SOI wafers would provide a material etch stop that gives a much higher control of the dimensions and higher yield. Future work will concern completing the characterization of the force sensor and performing a nanoindenter test with the sensors produced.

## 8 Recommendation for Further work

Even though a force sensor was designed and manufactured and the project is considered a success there are still some issues need to be changed and some investigated further to optimize the sensor, for example:

- Fabrication with a refined process plan using SOI wafers
- A more suitable evaluation system should be arranged and more tests run to characterize the sensor fully
- The alignment marks need to be redesigned with more care
- Investigate further the possibility to design an AFM and nanoindenter sensor in the same design if the diamond tip can be compromised with.

Ink. t Patent- och

2004-01-2

Huvudföreläsare

## 9 Acknowledgements

First of all I like to thank my supervisor Peter Enoksson at Solid State Electronics Laboratory at Chalmers along with Fredrik Althoff and Jens Dahlgren from Nanofactory Instruments and Håkan Olin at Mithögskolan in Sundsvall for making this project possible and for their support during the project.

Furthermore I like to thank Martin Bring, Anke Sanz-Velasco and Karin Hedsten for all their help and valuable advices, thank you all.

I also like to thank Christina Rusu at Imégo and Frank Lauterbach from Karl Suss for helping me in my struggle against the anodic bonding machine.

Finally, I am grateful to rest of the staff at the Solid State Electronics for making my time here enjoyable.

9  
2  
6  
1  
9  
2  
1

## 10 References

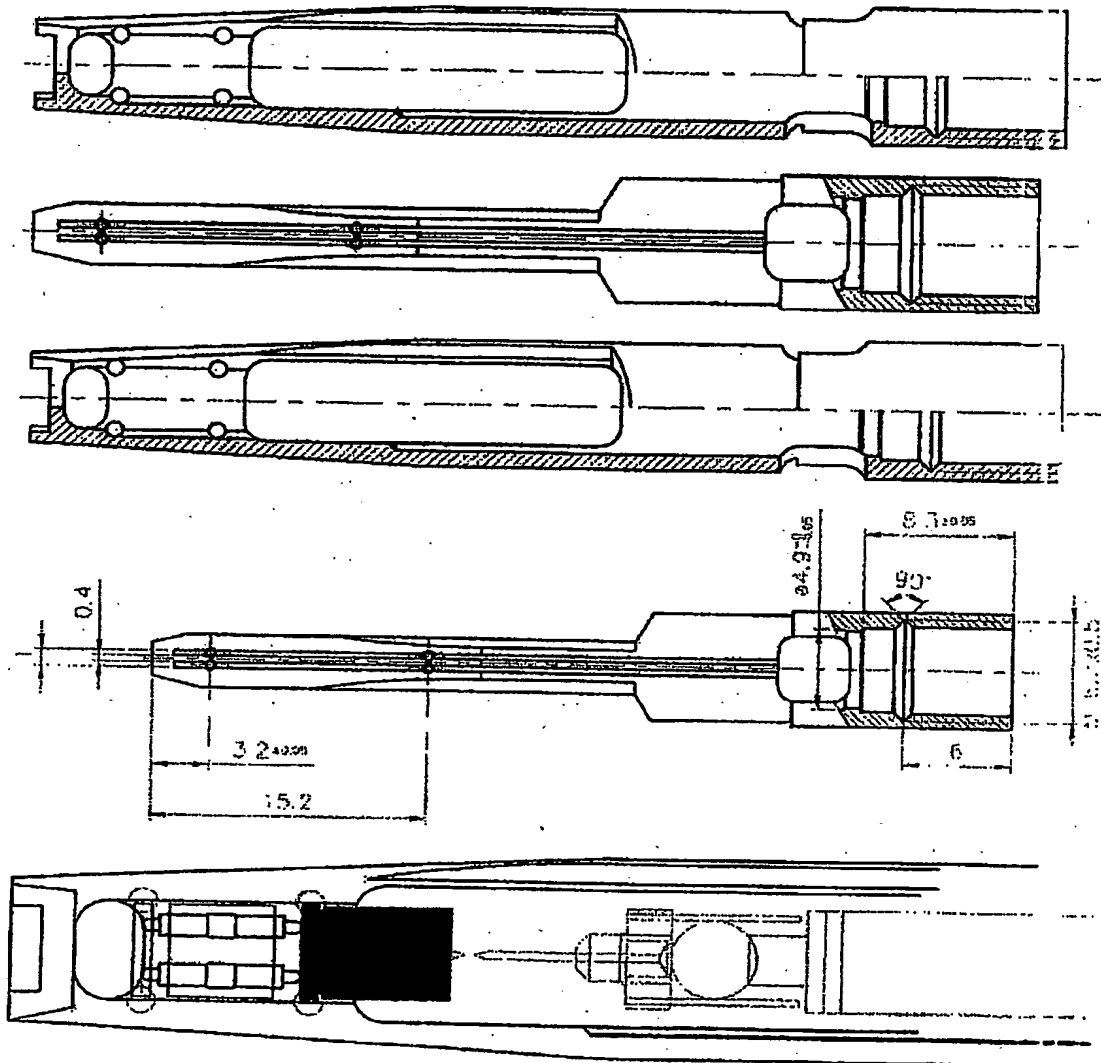
- [1] Kurt E. Petersen "Silicon as a Mechanical Material", Proceedings of the IEEE, Vol 70, no 5, pp. 420-457, 1982
- [2] A.M. Minor, J.W. Morris, Jr. and E.A. Stach "Quantitative in situ nanoindentation in a electron microscope" Applied Physics Letters, vol 79, nr 11
- [3] <http://www.nobel.se/physics/educational/microscopes/tem/>
- [4] Anthony C. Fischer-Cripps "Nanoindentation", published 2002, ISBN 0-387-95394-9
- [5] <http://www.tip.csiro.au/IMP/Surfaces/UMIS/Downloads/UMISBrochureMultiPage.pdf> page 4, 2003
- [6] "Micro indentation device for in situ study of pressure-induced phase transformation" Yury Gogotsi, Thomas Miletich, Michael Gardner and Michael Rosenberg, Review of Scientific Instruments Volume 70, number 12, December 1999
- [7] [http://www.mpikg-golm.mpg.de/gf/PhD\\_Sem.28.11.2003\\_Nils\\_Elsner.pdf](http://www.mpikg-golm.mpg.de/gf/PhD_Sem.28.11.2003_Nils_Elsner.pdf)
- [8] [http://www.mpiip-mainz.mpg.de/~jonas/Master\\_Surf\\_Chem/lecture\\_IntroSurfChem\\_2a\\_2.pdf](http://www.mpiip-mainz.mpg.de/~jonas/Master_Surf_Chem/lecture_IntroSurfChem_2a_2.pdf)
- [9] "Handbook of sensors and actuators" Volume 8, M. -H. Bao, published 2000, ISBN 0-444-50558-X
- [10] "A new force sensor incorporating force-feedback control for interfacial force microscopy" Stephen A. Joyce and J.E. Houston, Review of Scientific Instruments Vol: 62 710-715, 1991
- [11] S. M. Sze "VLSI Technology" published 1988, ISBN 0-07-100347-9
- [12] Richard C. Jaeger "Introduction to microelectronic fabrication", second edition volume V, published 2002, ISBN 0-201-44494-7
- [13] [http://www.minerals.sk.ca/atm\\_design/mirror\\_substrate.html](http://www.minerals.sk.ca/atm_design/mirror_substrate.html)

Ink: 1 Patent: not reg. v

1.1.1.1.2.6

Hauschilder, Krieger

# Appendix 1: CAD drawings of the holder



Ink. t. Patent- och reg.verd

2004-01-26

Huvudtaxen Kassan

## Appendix 2: Design layout

### Table of figures:

- Figure 1: The entire mask, each component is 1.5 mm by 2 mm
- Figure 2: Mask 1, inner fixture diameter 0.4 mm
- Figure 3: Mask 1, inner fixture diameter 0.45 mm
- Figure 4: Mask 1, safe design, inner fixture diameter 0.5 mm
- Figure 5: Mask 2, spring definition
- Figure 6: Mask 2, spring definition, an extra bend added
- Figure 7: Mask 3, glass recess and electrode trenches for one capacitance
- Figure 8: Mask 3, glass recess and electrode trenches for four capacitance
- Figure 9: Mask 4, electrode definition for one capacitance
- Figure 10: Mask 4, electrode definition for four capacitances

2004-01-26

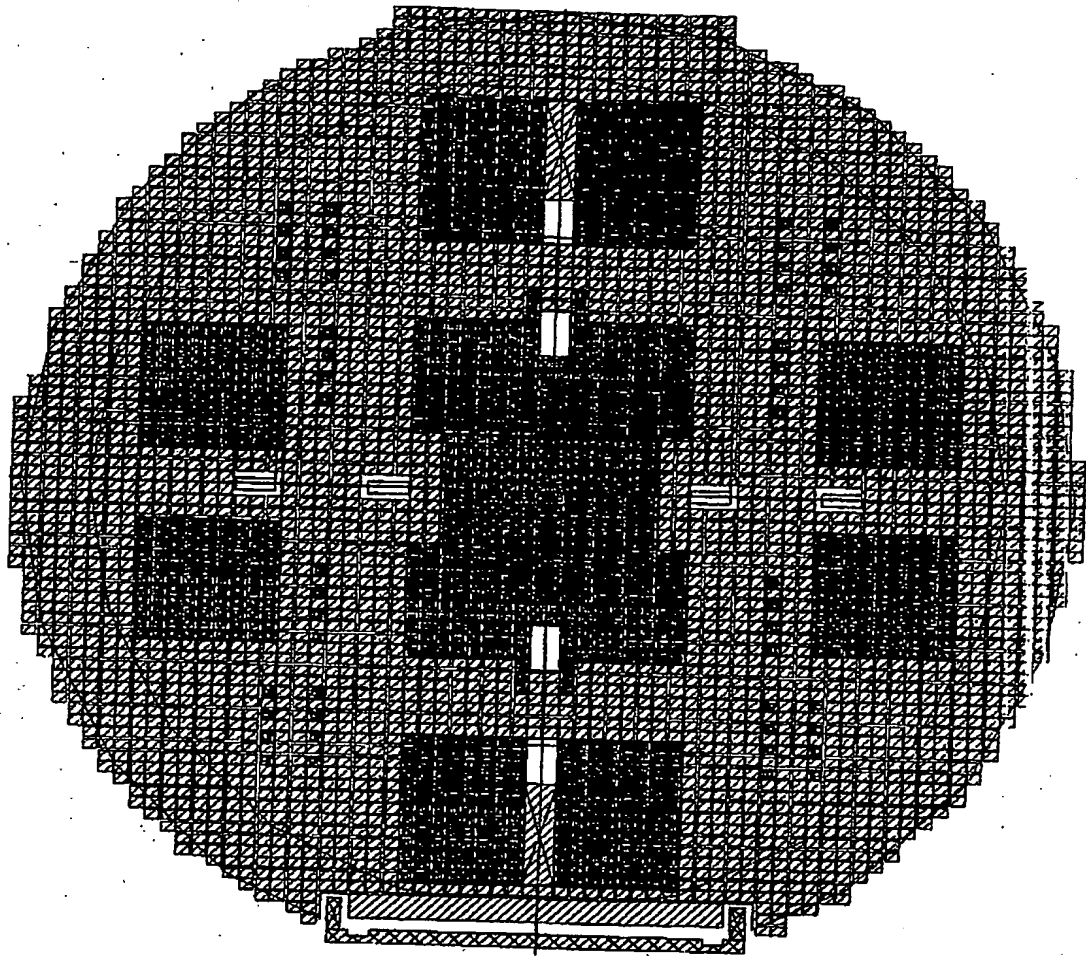


Figure 1: The entire mask, each component is 1.5 mm by 2 mm, about 1000 sensors

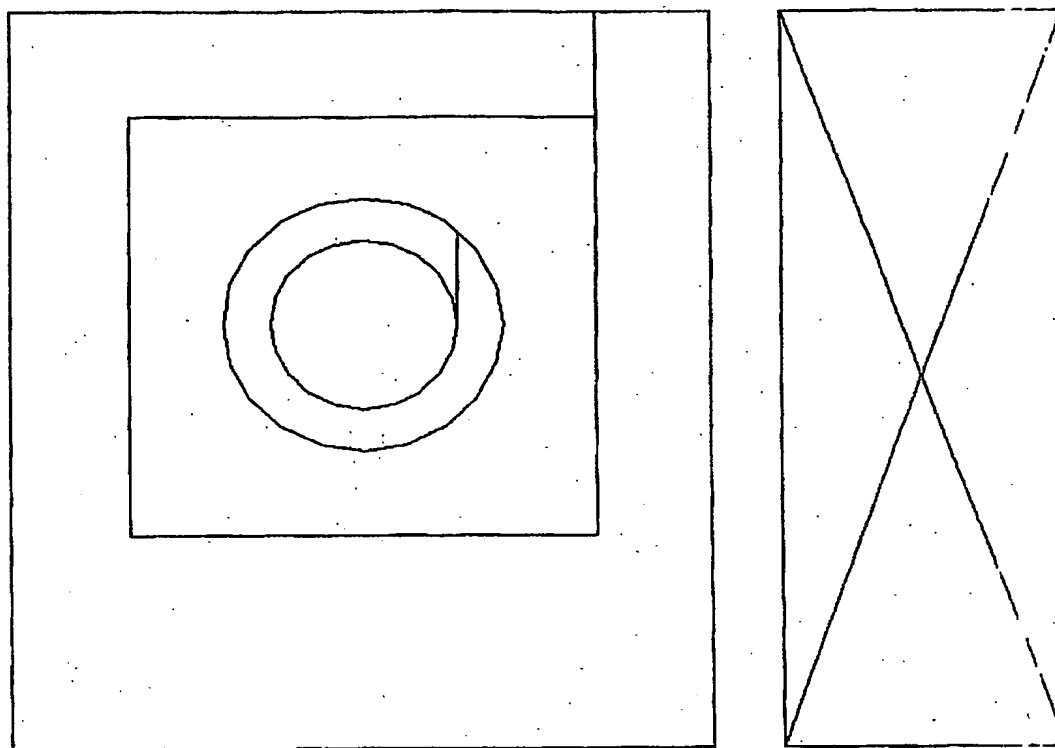


Figure 2: Mask number 1, holder etch. The diameter of the inner circle is 0.4 mm

0125000

Ink 1 Patent- och reg. vrd

2004-01-26

Huvudfuxen Kasson

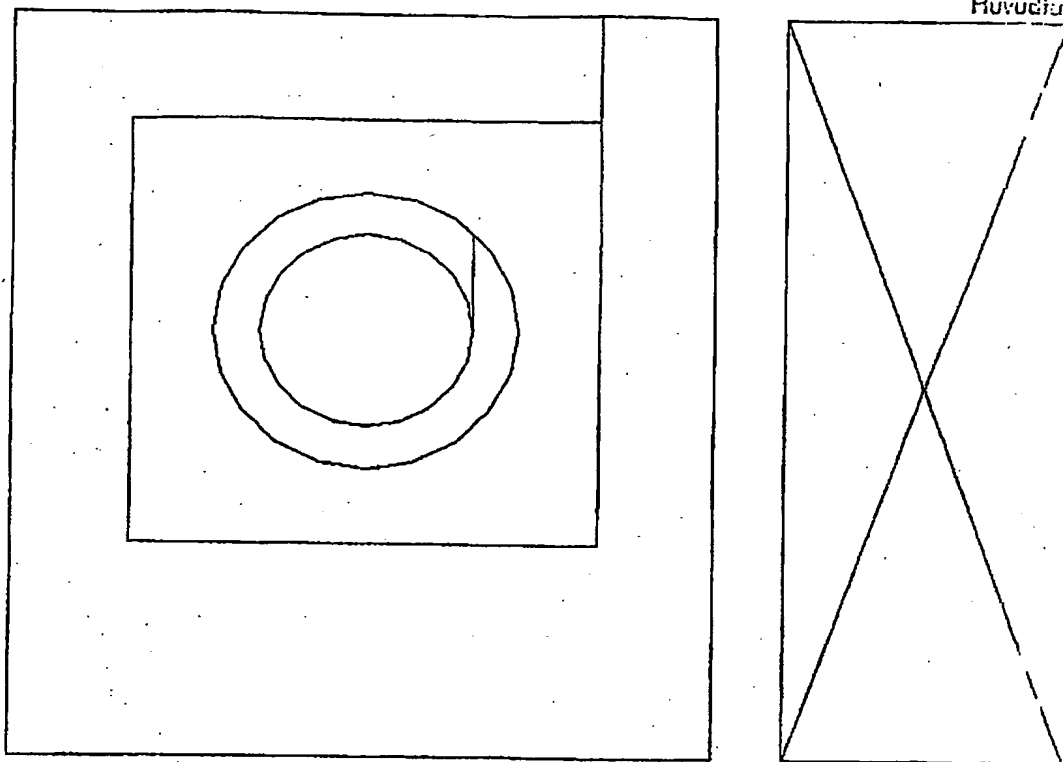


Figure 3: Mask 1, holder etch. The diameter of the inner circle is 0.45 mm



Ink. t. Patent- och registerverket

2004-01-26

Huvudföreläggningen

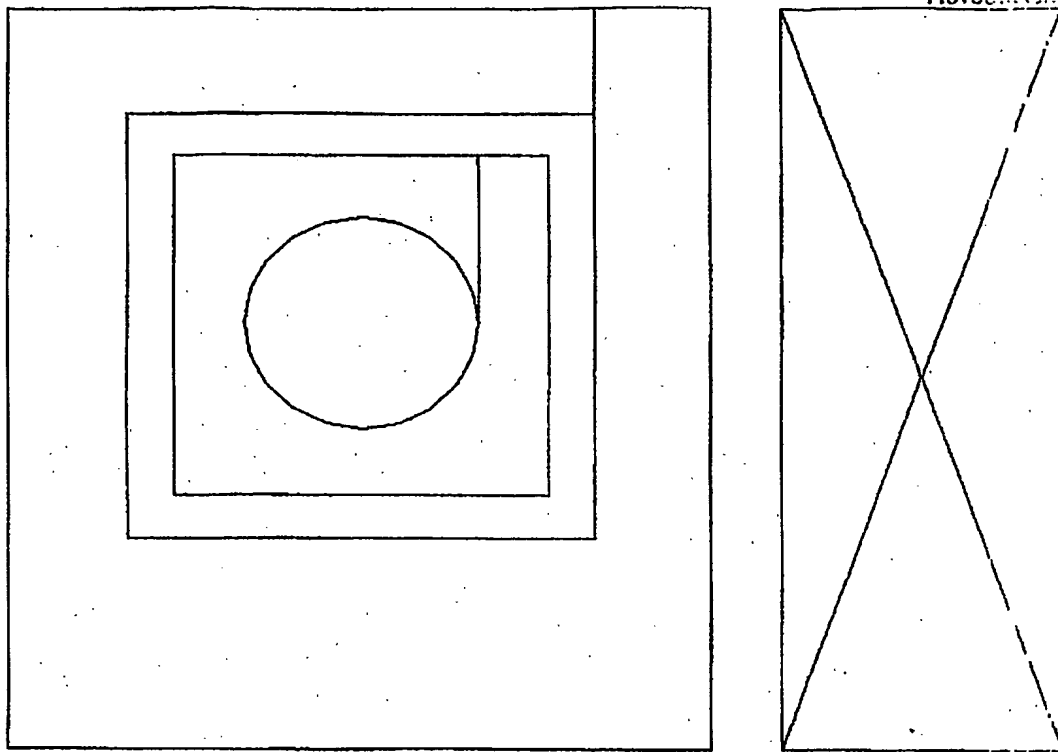


Figure 4: Mask 1, holder etch safe design. The diameter of the inner circle is 0.5 mm

2004-01-26





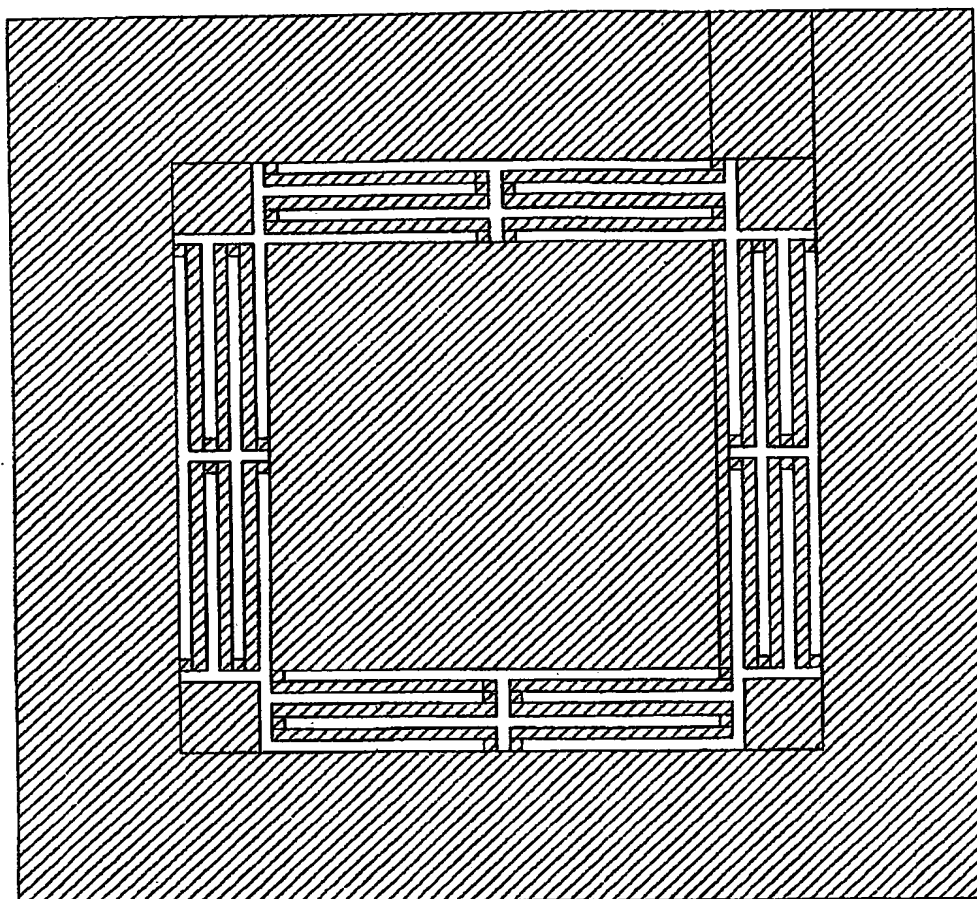


Figure 6: Mask 2, spring definition, springs with an extra bend

04005373

Ink t. Patent- och reg.verket

144 -01- 2 6

Huvudkontor Kåsan

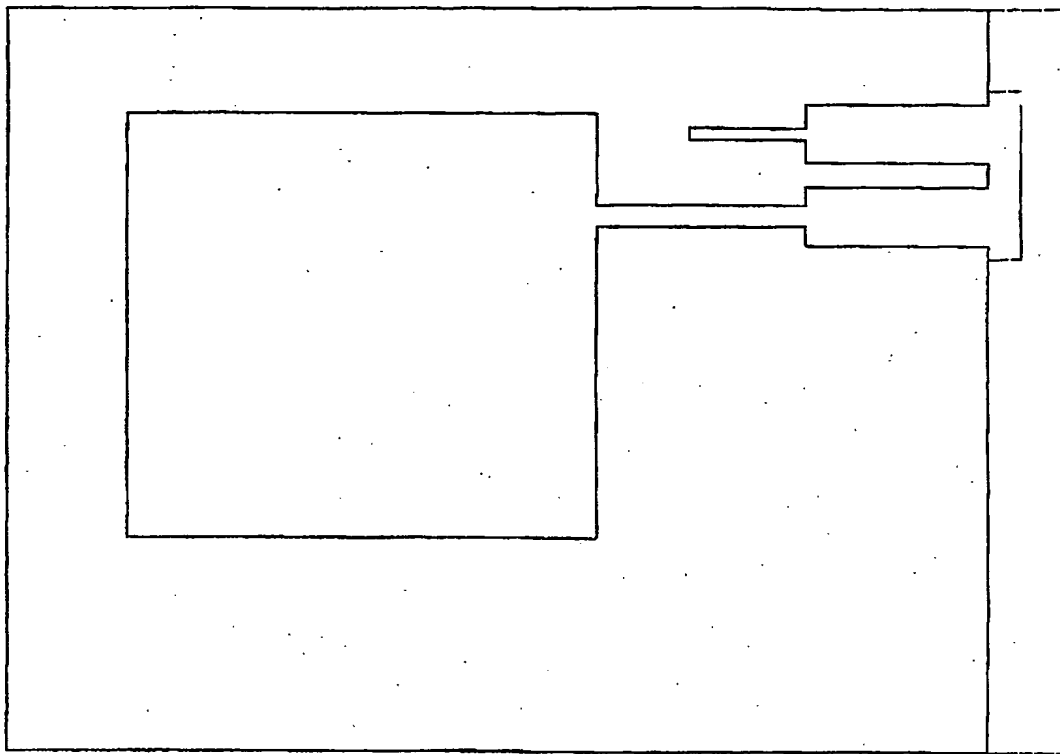


Figure 7: Mask 3, glass etch for one capacitance

0123456789

2004 01 26

Huvudkontor Kungälv

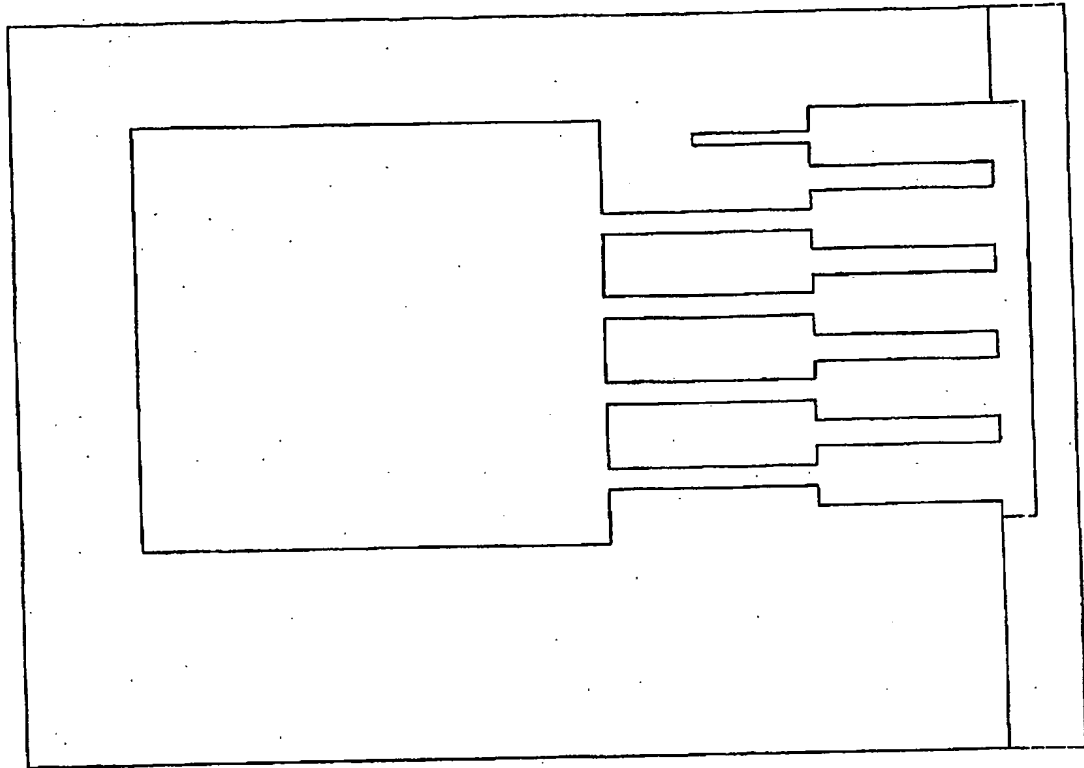


Figure 8: Mask 3, glass etch for four capacitances

0123456789

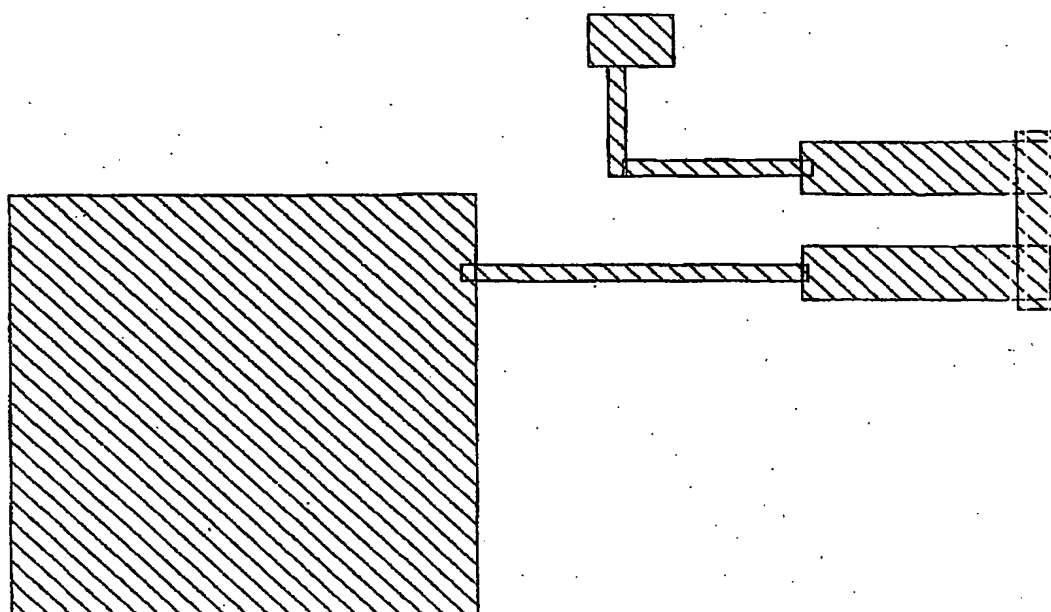


Figure 9: Mask 4, electrode definition for one capacitance

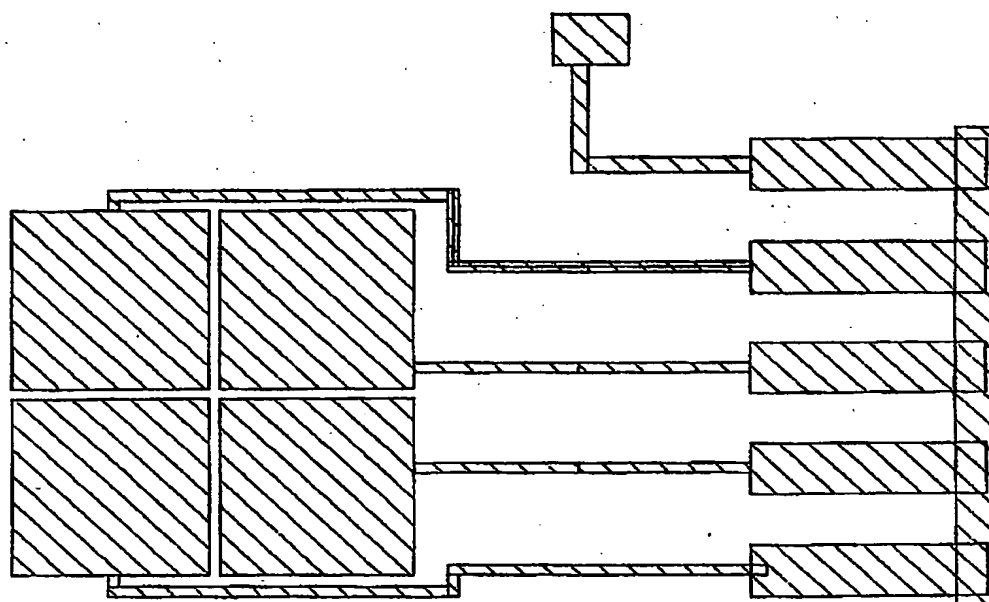


Figure 10: Mask 4, electrode definition for four capacitances

Ink t. Patent- och register

2004-01-26

Huvudstad: Stockholm

### Appendix 3: Anodic bonding

There were several tries done to find a working recipe to bond the processed silicon and glass wafers. The first problem encountered was the aligning. There is one universal chuck to use in the MC2 laboratory. The universal chuck has a vacuum hole in the middle and the vacuum is then distributed to the whole chuck through vacuum spirals. This means that the chuck cannot be used if the upper wafer has holes in it. In this case the vacuum could hold on to the silicon despite the holes in it but when the glass wafer was brought closer for alignment it stuck on the silicon wafer. The vacuum could keep the glass wafer stuck on the silicon through the holes. Luckily we had an opportunity to borrow another chuck from Karl Suss, this chuck had the vacuum at three holes at the edge of the wafer. The attempts described below were done with this chuck.

If this were known before the masks were done it would be possible to make the alignment marks so that the glass could be used as a top wafer, then the vacuum would not be a problem. There are however cases where it is not possible to have the glass as the top wafer for example when the silicon has very fragile structures on it. The tool pressure in the bonding machine is applied to the bottom wafer (the bottom wafer in the mask aligning = top wafer in bonding machine). A Karl Suss Bond Aligner (BA6) and Substrate Bonder (SB6) was used to perform the anodic bonding.

Attempt 1: Silicon to glass bonding, no alignment since the wafers were broken at one end

Parameters:

Temperature: 420 °C, ramp time 300 s  
Voltage: 200 V (-200 V on the glass), no ramp time  
Tool pressure: 100mBar  
Aluminium thickness: 1 µm  
Time: wait until the current increases and then has a dip ?

The bonding went well on open areas but it did not bond at all where the components were. A few components were bonded on the edges. It is hard to conclude anything since the wafer was not aligned.

Attempt 2: Silicon to glass bonding, aligned. The wafers were bonded three times.

The aluminium thickness is 1 µm in this attempt.

Parameters:

1. Temperature: 420 °C, ramp time 300 s  
Voltage: 200 V (-200 V on the glass), no ramp time  
Tool pressure: 100mBar  
Aluminium thickness: 1 µm

None of the components were bonded, the open areas bonded however well.

2. Temperature: 420 °C, ramp time 300 s  
Voltage: Started at 300 V, nothing happened so the voltage was increased, the maximum current

Ink. t. Patent- och reg.verket

2004-01-26

Hans-Joachim Karsen

level (15mA) was reached at 400 V. Then the voltage was slowly ramped up to 580 V  
 Tool pressure: 200mBar

It seems as if the temperature was too high, there were some brown stains on the glass wafer. The brown stains were later explained as used sodium ions that had reached the top electrode and were burnt there. To avoid the stains a dummy glass wafer can be placed on the top wafer in the bonding machine, the sodium ions will then wander through the top wafer to the dummy glass and the stains will not appear on the processed wafer. The wafers were slightly more bonded compared to the first time the wafers were bonded, but the components were still not bonded. The increased tool pressure had only a marginal effect. The aluminium looked a bit burned at the edges and in the middle.

3. Temperature: 390 °C, ramp time 300 s  
 Voltage: Put on as much voltage as possible, the limit was at 500 V. The current seemed very strange, it oscillated between 0 and 15 mA. The cables were checked and there was no problem there.  
 Tool pressure: 1 Bar

The idea to have 1 Bar in tool pressure was to if it is possible to mechanically apply the pressure needed to bond the wafer. The method was partially successful; there were rows of bonded areas in the component areas. In some places the glass wafer was bent and bonded to the silicon. Even though mechanical pressure can be used to help the bonding it is preferred to not use it. It is a destructive method; the glass wafer had some cracks on it after this procedure.

Attempt 3: Silicon to glass bonding, aligned.

The conclusion from the earlier is that the aluminium had to thinned. A thickness of 1  $\mu\text{m}$  is too much for anodic bonding. So the next aluminium evaporation on the glass wafer was targeted to 0.5  $\mu\text{m}$ . The resulting thickness was 0.7  $\mu\text{m}$ , which is still too thick so the aluminium thinned in aluminium etched to 0.45  $\mu\text{m}$ . This took 1 min 38 s using the aluminium etch bath in the laboratory at 40 °C, with agitation.

Parameters:

Temperature: 390 °C, ramp time 300 s  
 Voltage: 200, 250, 300, 400, 500, 600, 700, 800 V  
 600 V and 700 V were on in 30 min. The current was very low during the process, so the choices are then to wait longer or to increase the voltage. A combination was tried.  
 Tool pressure: 100 mBar  
 Aluminium thickness: 0.45  $\mu\text{m}$

The recipe worked very well. The devices looked very good, that means the walls on the devices bonded while the springs were free. On some of the components on the edges the springs was also bonded to the glass, the voltage used should have been a bit lower. To get better yield 600V should be used and the recipe should be set to wait at least 30 min. There is

Ink. t. Patent- och reg.verket

2004-01-26

Huvudfaxen, Kazan

a trick to change the maximum time each can be in the program. One can just change the alarm time in the recipe (in the middle of the process), save and load again.

THE UNIVERSITY OF CHICAGO

Ink. t. Patent- och reg.verket

2004-01-26

Huvudkontor Kassar

**Appendix 4: AFM and nanoindenter sensor calculation programs****The relative capacitance change for the nanoindenter design**

clear;

%Setting all the necessary constants

er=1;

eo=8.85e-12;

d=2.5e-6;

Ah=(0.4e-3)^2\*pi;

%5.0265e-007

Am=800e-6\*800e-6-Ah;

%1.3735e-007

A=Ah+Am;

%6.4000e-007

%Deflection from FEMLAB simulation is used

%and the relative capacitance is calculated

deltaD=[1.0225e-9 1.0225e-6];

C=eo\*er\*A\*deltaD./(d-deltaD)^2

%1.4479e-015 6.06e-12

C0=eo\*er\*A/d;

%2.2620e-012

**The resonance frequency and the spring constant calculation for the nanoindenter design**

%The mass of the sensor with and without the diamond tip is calculated

Vh=pi\*(0.3e-3)^2\*500e-6-pi\*(0.2e-3)^2\*500e-6;

%7.8540e-011

Vd=pi\*(0.2e-3)^2\*(0.4e-3+(1/3)\*0.3e-3);

%6.2832e-011

rho\_Si=2330;

rho\_d=3e3;

md=Vd\*rho\_d;

%1.8850e-007

mSi=Vh\*rho\_Si;

%1.8300e-007

m\_diamant=Vh\*rho\_Si+Vd\*rho\_d;

%3.7149e-007

m\_kisel=Vh\*rho\_Si;

%The diamond tip is 50% of the total mass

md\_proc=md/m\_diamant;

%0.5074

%The spring constant of the structure is calculated

%The resonance frequency is calculated including and excluding the diamond tip

deltaD=1.0225e-9;

F=0.1e-6/8;

k\_fjader=F/deltaD;

%1.2225e+001

k\_system=k\_fjader\*8;

%97

w0\_diamant=sqrt(k\_system/m\_diamant);

%1.6225e+004

f\_diamant=w0\_diamant/(2\*pi);

%2.5823e+003

w0\_kisel=sqrt(k\_system/m\_kisel);

%2.3118e+004

Ink t. Patent- och reg.verket

2004-01-26

Hans-Eriksson Karsen

```
f_kisel=w0_kisel/(2*pi); %3.6793e+003
```

### Relative resistance change for piezoresistive elements

```
E=131e9; %Youngs module
pi_p=138e-11; %piezoresistive coefficient for p-type silicon
pi_n=-102.2e-11; % piezoresistive coefficient
nu=0.27; %Poisson constant
h=[30e-6 20e-6 10e-6 5e-6]; %Membrane thickness
eps_sim=[9.4e-14 2.9e-13 7.72e-13 5.9e-12]; %Simulated strain

R_n=eps_sim.*(1+2*nu+pi_n*E) %Relative resistance change for n-type silicon
R_p=eps_sim.*(1+2*nu+pi_p*E) % Relative resistance change for p-type silicon
```

```
plot(h,R_p)
xlabel('membrane thickness')
ylabel('relative resistance change')
title('Change in resistance due to applied resolution force')
```

### The relative capacitance change for the AFM design

```
clear;
```

```
%Defining constants, d= distance between plates, A= area of the plate
```

```
er=1;
eo=8.85e-12;
d=2e-6;
Ah=(0.4e-3)^2*pi %5.0265e-007
Am=800e-6*800e-6 %1.3735e-007
A=Ah+Am %6.4000e-007
```

```
%Calculating the capacitance
```





```
deltaD=[ 3.1e-12 9.8e-12 7.7e-11];
C=e0*er*A*deltaD./(d-deltaD)^2 % 4.4e-018 1.4e-017 1.1e-016
C0=e0*er*A/d %2.8320e-012
```

Ink t. Patent- och reg. verkst.

074-01-2 G

Påsk. H. - J. K. K. K.

**Appendix 5: Process Plan for a Nanoindenter Force Sensor**

1. Substrate	1 Silicon wafer 6" Substrate thickness $540 \mu\text{m} \pm 10 \mu\text{m}$	 540 $\mu\text{m}$
2. Cleaning Si-wafer	Clean in SC1 for 10 min at 80°C (SC1: 5000 ml H <sub>2</sub> O, 1000ml NH <sub>3</sub> , 1000 ml H <sub>2</sub> O <sub>2</sub> ) Rinse 2 times in distilled water Dip in 2% HF for 30 sec Rinse 1 time in distilled water  Clean in SC2 for 10 min at 80°C (SC2: 5000 ml H <sub>2</sub> O, 1000 ml HCl, 1000 ml H <sub>2</sub> O <sub>2</sub> ) Rinse 2 times in distilled water Dip in 2% HF for 30 sec Rinse 1 time in distilled water Rinse and dry	
3. Oxidation	Grow oxides for mask Wet oxidation  Grow 2 $\mu\text{m}$ oxide on whole wafer Recipe: 15 h, 1050°C, standard Resulting thickness: 21 600 Å	
4. Lithography (MA6)	Front side lithography of Si-wafer  Spin HMDS Spin on resist AZ1512 at 3000 rpm for 30 s, with gyrset Softbake at 100°C for 1 min on hotplate Align with flat edge and expose for 2.7 s Develop with AZ312MIF: H <sub>2</sub> O (1:1) for approximately 30 s Rinse in distilled water once Rinse and dry	
Mask 1 Holder etch		

ink 1. Patent- och registerat

2004-01-26

Hälsning från KTH

Inspect in microscope  
 Hardbake at 120°C for 30 min in oven

Check mask and clean with acetone

## 5. Etch oxide

Etch the front and back oxide, 2µm

## Wet etch BOE

Etch in BOE 7944 (Buffered  
 Oxid Etch, 1100Å /min)  
 Etch for approx. 25 min or until  
 water pour of easily, due to hydrophobic  
 property of silicon

Resulting time: 27 min 33 s



## 6. Resist strip

Place in remover until all  
 resist is removed  
 Rinse for 5 min in distilled water  
 Rinse and dry  
 Inspect in microscope



## 7. Doping

Make P-type doping above  $10^{23}/m^3$ ,  
 Boron. Dope to 12 Ω/sq

Contact and  
 connection layer  
 to capacitance

"Constant source doping" Place dope  
 wafers on every third place since only  
 one side of the Si wafer is doped  
 Temp = 1040°C, Time = 30 min



## 8. Resist spinning

Spin resist on the oxide pattern, the top side  
 of the silicon wafer

Spin HMDS  
 Spin on resist AZ4562 at 3000 rpm  
 for 30 s, with gyrset  
 Softbake at 100°C for 3 min on hotplate  
 Hardbake at 120°C for 60 min in oven



## 9. Remove boroxide

Wet etch BOE Etch in BOE 7944 (Buffered  
 Oxid Etch, 1100Å /min)  
 Etch for approx. 7 min or until  
 water pour of easily



EK 12-01-00-00-00-00

100-01-00-00-00-00

100-01-00-00-00-00

Resulting time: 7 min 45 s

**10. Resist strip**

Place in remover until all  
resist is removed  
Rinse for 5 min in distilled water  
Rinse and dry  
Inspect in microscope

**11. Doping concentration**

Measuring the doping

Resulting doping level: 40  $\Omega/\text{sq}$ **12. Lithography**

Backside lithography of the Si-wafer

Mask 2  
Spring etch

Spin HMDS  
Spin on AZ4562HS at 3000 rpm for 20 s,  
with gyrset, target thickness= 4 $\mu\text{m}$   
Softbake at 100 °C for 3 min on hotplate  
Align with flat edge and expose for 25 s  
Develop with AZ312MIF: H<sub>2</sub>O (1:1)  
for approx. 3 min in 30 s  
Put in distilled water for 2 min  
Dryblow with N<sub>2</sub>  
Inspect in microscope  
Hardbake at 120 °C for 60 min in oven



Check mask and clean with acetone

**13. Silicon etch**Etch SI-wafer with STS ICP RIE, 40  $\mu\text{m}$ 

Shallow dry  
etch

ICP recipe: Si\_slow  
Test etch for 5 min  
Measure etch depth in Tencor  
Calculate etch speed at edge



Perform complete ICP etch for another X min  
Total etch time: 13+5 min  
Resulting etch: 38  $\mu\text{m}$  – 41  $\mu\text{m}$   
Etch rate: about 2.5 $\mu\text{m}/\text{min}$

**14. Resist strip**

Place in remover until all  
resist is removed  
Rinse for 5 min in distilled water  
Rinse and dry



Litho: Front-side registration

1-01-26

Front-side lithography

## Inspect in microscope

## 15. Lithography

Front side lithography of Si-wafer,  
to enhance the oxide pattern



Mask 1  
Holder etch

Spin HMDS  
Spin on resist AZ4562 at 2000 rpm  
for 25 s, with gyrset => 8µm resist  
Softbake at 100°C for 3 min on hotplate  
Align with flat edge and expose for 35 s  
Develop with AZ312MIF: H<sub>2</sub>O (1:1) for  
approximately 3 min 30 s  
Rinse in distilled water once  
Rinse and dry  
Inspect in microscope  
Hardbake at 120°C for 60 min in oven

Check mask and clean with acetone

To strengthen the oxide for deep etch

## 16. Silicon etch

Deep ICP etch of Si  
Oxide mask



Dry etch

ICP recipe: Si\_slowo, approx 3 µm/min

Test etch for 10 min  
Measure etch depth in Tencor  
Calculate etch speed at edge

Perform complete ICP etch for another X min  
Total etch time: 10 min + 3 h 5 min  
Resulting etch rate: 2.8 µm/min

## 17. Resist strip

Place in remover until all  
resist is removed  
Rinse for 5 min in distilled water  
Inspect in microscope



## 18. Etch oxide

Oxide etch of the front side,  
2µm



Wet etch BOE

Etch in BOE 7944 (Buffered  
Oxide Etch, 1100Å /min)  
Etch for approx. 25 min or until water pour  
of easily

Resulting time: 20 min

Int. 1. Patent not registered

2004-01-26

Hauptstadt: Berlin

19. Cleaning  
Si-wafer

Clean in SC1 for 10 min at 80°C  
(SC1: 5000 ml H<sub>2</sub>O, 1000ml NH<sub>3</sub>,  
1000 ml H<sub>2</sub>O<sub>2</sub>)

Rinse 5 times in distilled water

**Do not flush with water**

Dip in 2% HF for 30 sec

Rinse 2 time in distilled water

Place the wafer carefully in a beaker with IPA for 10 min

Move the wafer to a new beake with IPA to minimize  
the risk of having any HF left in the wafer, for 5 min.

Dry carefully and make sure that it is dry



## 20. Substrate

1 Pyrex wafer 6"

Substrate thickness 500 μm ± 15 μm

Pyrex Glass

500 μm

## 21. Lithography

Lithography on the front side of  
the glass

Mask 3

Glass cavity

Spin HMDS

Spin on AZ4562HS at 2000 rpm for 30 s,  
with gyrset => 8.7 μm resist

Softbake at 100 °C for 3 min on hotplate

Align with flat edges and expose for 45 s

Develop with AZ312MIF: H<sub>2</sub>O (1:1) for 3 min 30 s

Put in distilled water for more than 2 min

Dryblow with N<sub>2</sub>

Inspect in microscope

Hardbake at 120°C for 60 min in oven

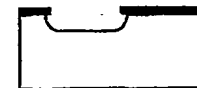
Check mask and clean with acetone

22. Etch bonding  
glass

Etch the glass wafer, 3 μm

Wet etch

Etch in concentrated HF, 49%, for 23s  
About 7μm/min,



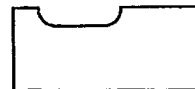
Link 1: Patent - not recommended

7-1-01-26

Result: 2.8  $\mu\text{m}$ Result: 2.8  $\mu\text{m}$ 

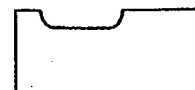
## 23. Resist strip

Place in remover until all  
resist is removed  
Rinse twice in distilled water  
Rinse and dry  
Inspect in microscope



## 24. Cleaning glass wafer

Clean in SC1 for 10 min at 80°C  
(SC1: 5000 ml H<sub>2</sub>O, 1000ml NH<sub>3</sub>,  
1000 ml H<sub>2</sub>O<sub>2</sub>)  
Rinse 2 times in distilled water



## 25. Aluminum evaporation

Evaporate 5 000 Å aluminum on glass  
wafer

Equipment used: Evaporator Balzer

Electrodes  
deposition

Resulting thickness: 7 300 Å



## 26. Lithography

Lithography of the glass wafer

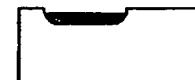
Mask 4  
Electrode mask

Spin HMDS  
Spin on AZ4562HS at 3000 rpm  
for 25 s, with gyrset  
Softbake at 100 °C for 3 min on hotplate  
Align with pattern and expose for 30 s  
Develop with AZ312MIF: H<sub>2</sub>O (1:1) for  
approx. 3 min 30 s  
Put in distilled water for more than 2 min  
Dryblow with N<sub>2</sub>  
Inspect in microscope  
Hardbake at 120 °C for 60 min in oven

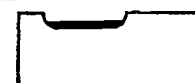
Check mask and clean with acetone

## 27. Aluminum etch

Etch aluminum for electrode



Etch in standard aluminum etch,  
approx. aluminum thickness 7 300 Å  
Etch until no Al is left  
Resulting time: about 8 min, using only agitation



Ink. t. Patent- och reg.verket

7-1-01-26

Här till: Kasean

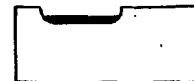
**28. Resist strip**

Place in remover until all  
resist is removed  
Rinse twice in distilled water  
Rinse and dry  
Inspect in microscope

**29. Cleaning  
glass wafer**

Clean in acetone for 5 min  
Rinse and dry

**Do not clean in SC1, the chemicals will  
dissolve aluminum**

**30. Anodic bonding**

Wafer bond the processed silicon to the  
processed glass wafer

Temperature: 390 °C

Voltage: Increase from 200-700 V wait at  
600 V and 700 V for 30 min

Tool pressure: 100 mBar

Spacers used during alignment

Appendix 4 contains a more detailed description

**31. Saw individual  
Structures**

Mount the wafer on tape with the  
silicon facing down. Use the saw  
marks to aim the blade.  
The saw blade called 1002 with a thickness  
of 100 µm was used

It can be convenient to saw the wafer into several parts and  
then saw out each component



54